EFFECT OF PRE-AGEING THERMAL CONDITIONS ON THE HARDNESS, CORROSION RESISTANCE AND MICROSTRUCTURAL MORPHOLOGY OF ANTIMONY MODIFIED Al-Si-Mg ALLOY

BY

GANIYU OLUSHOLA ADEBOYE

DEPARTMENT OF METALLURGICAL AND MATERIALS ENGINEERING

AHMADU BELLO UNIVERSITY, ZARIA,

NIGERIA

MAY, 2014

EFFECT OF PRE-AGEING THERMAL CONDITIONS ON THE HARDNESS, CORROSION RESISTANCE AND MICROSTRUCTURAL MORPHOLOGY OF ANTIMONY MODIFIED Al-Si-Mg ALLOY

BY

Olushola Ganiyu ADEBOYE B.Eng.(A.B.U), 2000
M.Sc./ ENG/ 05626/2010-2011

A THESIS SUBMITTED TO THE SCHOOL OF POSTGRADUATE STUDIES, AHMADU BELLO UNIVERSITY, ZARIA. IN PARTIAL FULFILMENT OF THE REQUIREMENTS FOR THE AWARD OF MASTERS DEGREE IN METALLURGICAL AND MATERIALS ENGINEERING

**DEPARTMENT OF METALLUGICAL ANDMATERIALS ENGINEERING,
FACULTY OF ENGINEERING,
AHMADU BELLO UNIVERSITY, ZARIA.**

MAY, 2014

DECLARATION

I hereby declare that the work reported in this thesis entitled **"Effect of Pre-ageing Thermal Conditions on the Hardness, Corrosion Resistance and Microstructural Morphology of Antimony Modified Al-Si-Mg Alloy''** has been performed by me in the Department of Metallurgical and Materials Engineering under the supervision of Dr. M. Abdulwahab and Prof. S.A. Yaro.

The information derived from literature has been duly acknowledged in the text and a list of references provided. No part of this thesis was previously presented for another degree or diploma at any University.

_____ _____

Name of student Signature Date

CERTIFICATION

This thesis entitled "EFFECT OF PRE-AGEING THERMAL CONDITIONS ON THE HARDNESS, CORROSION RESISTANCE AND MICROSTRUCTURAL MORPHOLOGY OF ANTIMONY MODIFIED Al-Si-Mg ALLOY'' by Olushola Ganiyu ADEBOYE meets the regulations governing the award of the degree of Masters of Science (Metallurgical and Materials Engineering) in Ahmadu Bello University, Zaria, and is approved for its contribution to scientific knowledge and literary presentation.

_____ _____

Dr. M. Abdulwahab
Chairman, Supervisory Committee Date

_____ _____

Prof. S.A Yaro
Member, Supervisory Committee Date

_____ _____

Prof. S.A Yaro
Head of Department Date

_____ _____

Prof. A. A Joshua
Dean, School of Postgraduate Studies Date

DEDICATION

This thesis is dedicated to the Almighty God who is the fountain of Knowledge.

ACKNOWLEDGEMENT

I cannot but thank the Almighty God for His grace, unquantifiable mercies, love and faithfulness at the course of this study. I greatly appreciate the efforts of my Supervisors Dr. M. Abdulwahab and Prof. S.A. Yaro, for their patience, sacrifices, commitments, supports and guidance in terms of thorough supervision, valuable and constructive inputs at every stage of this work. God will reward you bountifully.

My gratitude also goes to the members of staff of the Department of Metallurgical and Materials Engineering who made themselves available whenever I needed guidance. May you all see the goodness of the Lord in your entire endeavour.

I will not fail to appreciate the unrelenting efforts and immense contributions of my family members: Mrs Moriatu Adeboye, Alh. Isa Adeboye, Dr. (Arc.) and Mrs A.B. Adeboye, Mrs. S.O. Salami, Chief S.O. Adeboye, Pst. D.O. Adeboye, Precious Adeboye, Treasure and Triumph Adeboye, Ibrahim Olatunde and Miss Tope Sherifat Kadir for their prayers, encouragements and support throughout my study.

My special appreciation also goes to my friends and classmates, Samson Olajide (Sonite), Tayo Ige, Arobuwa Emmanuel, Saliu Zainab, Makanjuola Komolafe, Magagi Adefunke, Sis. Glory Kemi, Mrs Aina Shobayo, Modibo, Masok, for their hands of friendship and support. This study would most likely have been very boring and the journey 'long' without you being around. God bless you all.

Finally, I am particularly grateful to Mr Moses Simeon, Alh. Isiaka Ajibola and Mal. R.B. Musa, for given me useful advice and encouragements, financial and moral supports. May your greatness know no limits and may you reap the fruits of your labour.

ABSTRACT

The effect of pre-ageing thermal conditions on the hardness, corrosion resistance and microstructural morphology of antimony modified Al-Si-Mg alloy has been studied. The thermal treatment employed were Double Thermal Ageing, T7 (DTAT) comprising of pre-ageing temperatures of 90^0C, 105^0C and 120^oC with variable pre-ageing time of 1-5 hrs respectively, along with Single Thermal Ageing (STAT). The result of the average HRF hardness values show that, the hardness of the treated alloy DTAT conducted gave better hardness value compared with those obtained in the convectional STAT. The DTAT treatment increased the hardness by 67.0% as compared to 21.9% obtained for STAT treatment. The X-Ray Diffractometry (XRD) revealed that $Al_3Mg_7Si_2$, $Al_8FeMg_3Si_6$, Al_9Si and FeSi phases were present in the As-cast and Mg_2Si, Al_9Si, FeSi, Al_3Si_3 and $Al_{12}Mg_{17}$ phases were present in the treated alloy. For DTAT treatment, ageing at 90^0C has been observed to be the peak ageing temperature at 2hrs which gave a maximum value of 8.40HRF. Equally the alloys aged at 90^0C for 1hr and 120^0C for 1hr gave hardness value of 7.80HRF and 7.70HRF respectively for what could be attributed to the very fine coherent intermetallic precipitates which impede dislocation movement. The corrosion characteristic of as-cast, STAT and DTAT were evaluated using weight loss and electrochemical potentiodynamics techniques. From the linear polarization data and curves, the corrosion rate of the treated alloy decreases at all ageing temperatures along with the ageing time. The Optical microscope (OPM) results of as-corroded samples revealed that the alloy suffers pitting/uniform corrosion. The corrosion behaviour of the DTAT samples in simulated sea water showed a higher improvement in corrosion resistance than the as-cast and conventional STAT alloy.

TABLE OF CONTENTS

TITLE PAGE - - - - - - - - - - .i

DECLARATION- - - - - - - - - - - ii

CERTIFICATION - - - - - - - - - - iii

ACKNOWLEDGEMENTS - - - - - - - - iv

ABSTRACT - - - - - - - - - - v

TABLE OF CONTENTS - - - - - - - - - vi

LIST OF FIGURES - - - - - - - - - vi

LIST OF TABLES - - - - - - - - - viii

LIST OF PLATES - - - - - - - - - vii

LIST OF APPENDICES/ABBREVATIONS - - - - - - - viii

INTRODUCTION

1.1.1 Introduction - - - - - - - - - 1

1.1 Justification of the study - - - - - - - 3

1.2 Aims and Objectives - - - - - - - - 3

1.3 Scope of the study - - - - - - - - 4

1.4 Contribution to knowledge - - - - - - - 4

LITERATURE REVIEW

2.0 Literature review - - - - - - - - 5

2.1 Classification and designation of aluminum alloys - - - - 5

2.1.1 Classification - - - - - - - - - 5

2.1.2 Designation of aluminum alloys - - - - - - - 6

2.1.2.1 Cast aluminum - - - - - - - - - 7

2.2 Ternary phase diagram of Al-Si-Mg alloy- - - - - 8

2.3 Heat-treatable aluminum alloy - - - - - - - 9

2.4 Precipitation hardening heat treatment - - - - - - 9

2.4.1 Solution heat treatment - - - - - - - 10

2.4.2 Precipitation hardening- - - - - - - - 11

2.5 The effect of alloying element on the mechanical properties,

microstructures and age-hardening response of aluminum alloys - - 12

2.5.1 Eutectic Modification of Al-Si-Mg alloys - - - - - 14

2.6 Corrosion properties of aluminum and its alloys - - - - - 14

2.7 Applications of aluminum based alloys - - - - - - 17

MATERIALS AND METHODS - - - - - - - - 18

3.0 Materials and methods - - - - - - - - 18

3.1 Materials - - - - - - - - - 18

3.1.1 Equipment - - - - - - -- - - 18

3.2 Methods - - - - - - - - - 18

3.2.1 Casting of the samples - - - - - - - - 18

3.2.1 Heat treatment - - - - - - - - - 19

3.2.1.1 Single thermal ageing treatment (STAT-T6) - - - - - 19

3.2.1.2 Double thermal ageing treatment (DTAT-T7) - - - - - 19

3.2.2 Hardness measurement - - - - - - - 20

3.2.3 X-ray diffractometry (XRD) measurement - - - - - 21

3.2.4 Corrosion characteristics - - - - - - - 21

3.2.4.1 Weight loss technique - - - - - - - - 21

3.2.4.2 Electrochemical potentiodynamics technique - - - - - 21

3.2.3 Corrosion rate measuring techniques- - - - - - - 22

3.4.5 Microstructural examination - - - - - - - 23

RESULTS AND DATA PRESENTATION - - - - - - - 24

4.0 Results and Data presentation - - - - - - - 24

DISCUSSIONS - - - - - - - - - - 35

5.0 Discussions - - - - - - - - - - 35

5.1.1 Hardness measurement and thermal ageing treatments - - - - 35

5.1.1.1 Single Thermal Ageing (STAT) and Double Thermal Ageing

(DTAT) Treatments - - - - - - - - 35

5.2.1 Relationship between microstructure and hardness characteristics of the

studies Al-Si-Mg alloy - - - - - - - - 36

5.2.2 Corrosion characteristics - - - - - - - - 36

5.2.2.1 Linear polarization, STAT and DTAT treatment - - - - - 36

5.2.3 Microstructure and degradation of Al-Si-Mg alloy

after electrochemical corrosion attack - - - - - - 38

SUMMARY, CONCLUSION AND RECOMMENDATIONS

6.0 Summary, conclusion and recommendations- - - - - - 40

6.1 Summary - - - - - - - - - - 40

6.2 Conclusion - - - - - - - - - - 41

6.3 Recommendation - - - - - - - - - 42

REFERENCE - - - - - - - - - - 43

APPENDICES - - - - - - - - - 50

LIST OF FIGURES

Figure 2.1: Liquid surface of the ternary system Al-Si-Mg - - - - 8

Figure 2.2: Ternary Phase diagram for a composition base for an ABC - - 8

Figure 3.1: Schematic diagrams of STAT and DTAT heat treatment - - 20

Figure 4.1: Variation of hardness with ageing time of Al-Si-Mg alloy after Preaging at 90^0C,105^0C,120^0C- - - - - 28

Figure 4.2: Variation of Corrosion rate with ageing time for As-cast, STAT-T6 and DTAT-T7 A356.0-Type Al-Si-Mg Alloy at 90^0C from the weight loss plot data in Simulated Seawater Environment - - - - 28

Figure 4.3: Variation of Corrosion rate with ageing time for As-cast, STAT-T6 and DTAT-T7 A356.0-Type Al-Si-Mg Alloy at 105^0C from the weight loss plot Data in Simulated Seawater Environment - - - - 29

Figure 4.4: Variation of Corrosion rate with ageing time for As-cast, STAT-T6 and DTAT-T7 A356.0-Type Al-Si-Mg Alloy at 120^0C from the weight loss plot Data in Simulated Seawater Environment - - - - 29

Figure 4.5: Potentiodynamic polarization curves of thermally pre-aged Al-Si-Mg alloy at 90^0C in 3.5% NaCl solution at 25^0C - - - 30

Figure 4.6: Potentiodynamic polarization curves of thermally pre-aged Al-Si-Mg alloy at 105^0C in 3.5% NaCl solution at 25^0C - - - 30

Figure 4.7: Potentiodynamic polarization curves of thermally pre-aged Al-Si-Mg alloy at 105^0C in 3.5% NaCl solution at 25^0C - - - 31

Figure 4.8: XRD pattern A356.0-type Al-Si-Mg alloy for as-cast - - - - 31

Figure 4.9: XRD pattern of thermal treated A356.0-type Al-Si-Mg alloy for DTAT

(90^0C/1hr) - - - - - - - - 32

LIST OF TABLES

Table 2.1: Aluminum Alloy Designation Systems for Wrought Alloys - - - 6

Table 2.2: Aluminum Alloy Designation Systems for Casting Alloys - - - 7

Table 3.1: Chemical Composition of the produced Al-Si-Mg Alloy (wt %) - - - 19

Table 3.2: Summary of Sample Number, Analysis and Properties for Al-Si-Mg

Alloy Studied- - - - - - - - - 19

Table 4.1: Average HRF value measurement - - - - - - 24

Table 4.2: Linear polarization data of thermally pre-aged Al-Si-Mg alloy

at 90^oC in 3.5%NaCl solution at 25^0C - - - - - - 25

Table 4.3: Linear polarization data of thermally pre-aged Al-Si-Mg alloy

at 105^oC in 3.5%NaCl solution at 25^0C - - - - - 26

Table 4.4: Linear polarization data of thermally pre-aged Al-Si-Mg alloy

at 120^oC in 3.5%NaCl solution at 25^0C - - - - - 27

Table 4.5: Corrosion Rate of As-cast, STAT and DTAT (at 90^0C Pre-aging tempt.)

in 3.5% NaCl Over exposure time (hours) - - - - - 50

Table 4.6: Corrosion Rate of As-cast, STAT and DTAT (at 105^0C Pre-aging tempt.)

in 3.5% NaCl Over exposure time (hours) - - - - - 51

Table 4.7: Corrosion Rate of As-cast, STAT and DTAT (at 120^0C Pre-aging tempt.)

in 3.5% NaCl Over exposure time (hours) - - - - 52

LIST OF PLATES

Plate I: SEM micrograph with the EDS spectrum for As-cast sample - - - 32

Plate II: SEM micrograph and EDS spectrum for 90^0C/2hr sample - - - 33

Plate III: As cast structure Al-Si-Mg alloy - - - - - - - - 33

Plate IV: Antimony modified Al-Si-Mg alloy - - - - - - 33

Plate V: As corroded at 20^{th} day - - - - - - - - - 34

Plate VI: As corroded at 30^{th} day- - - - - - - - - 34

Plate VII: As corroded at 40^{th} day - - - - - - - 34

LIST OF ABBREVIATIONS, NOTATIONS AND UNITS

DTAT – T7 temper which involves solution heat treatment and slow precipitation for lower time combined with ageing for stabilization.

STAT – T6 tempered which involves solution heat treatment and slow precipitation for lower time combined with convectional ageing.

HRF – Rockwell hardness-F scale hardness value

K – Kelvin (^{0}C + 273)

hr – Hour

T5 – Artificially aged from the as-cast condition

T6 – Solution heat treated + artificial ageing (STAT)

T7 – Solution heat treated + artificial ageing for stabilization (Pre-ageing + artificial ageing)

XRD – X-Ray Diffraction

SEM-EDS – Scanning electron microscopy equipped with electron dispersive spectroscopy

OPM – Optical microscopy

Al-Si-Mg alloy – Aluminum + Silicon + Magnesium alloy

Al-Si alloy – Aluminum + Silicon alloy

CHAPTER ONE

1.0 INTRODUCTION

Al-Si-Mg alloys are groups of heat treatable cast Al-Si alloys (Zou *et al.*, 2010 and Kumar *et al.*, 2007), which after fabrication, needs an artificially ageing heat treatment to attain the desired strength (Perez, 2011 ; Reddy and Rao, 2010).The alloys have a wide range of applications in the automobile and aerospace, defense and general engineering industries (Imurai *et al.*, 2010). A356 (Al-7Si-0.3Mg) and A357 (Al-7Si-0.5Mg) series are the two commonly used Al-Si-Mg alloys (Li *et al.*, 2006) used to obtain near net shape products (Tahamtan and Boostani, 2010) because of its high fluidity and good castability (Kuntongkun *et al.*, 2008) owning to the high volume of Al-Si eutectic, in the microstructure.

Castings made of Al-Si-Mg alloy exhibit many benefits such as good wear and corrosion resistance (Jenabali *et al.*, 2004), hot tearing resistance (Alcan, 2007) i.e. resistance to separation of the already crystallized phases during solidification (www.aleris.com), good weldability, increased energy efficiency (Jiang *et al.*, 2011), good tensile strength (Leo and Cerri, 2003) and high strength to weight ratio (Pio, 2011) which increases performance and fuel economy (Morri, 2010) .The mechanical properties of the Al–Si–Mg alloys are determined by solidification rate, as-cast microstructure, integrity and heat treatment (Hitchcock *et al.*, 2007). Hence, the reliability and functionability of casting products are very much dependent on the mechanical properties of Al-Si alloys in the as-cast condition. However, some mechanical properties of the Al-Si-Mg cast alloy, in particular, ductility, toughness and corrosion resistance, are affected by the morphology and distribution of the second phases (Zou *et al.*, 2010). The commonly practiced methods for enhancing the mechanical properties of Al-Si castings are grain refinement, modification and precipitation heat treatment (Kumar *et al.*, 2007). Grain refinement is by the addition of Ti-B or Ti-C based grain refiners into the melt to refine the grain size of the casting to a fine equiaxed grain (Zhang *et al.*, 2005) and to enhance the metal stability (Gbenebor *et al.*, 2012) while

modification is by the inoculation of the melt with modifiers containing strontium, sodium, antimony and rare earth elements to modify the eutectic silicon phase from coarse and plate-like to fine and fibrous morphology (Chen *et al.*, 2012). A356 and A357 alloys have Si and Mg as the principal alloying additions to aid in the precipitation of the Mg_2Si phase in the primary matrix to strengthen the alloys during heat treatment (Abdulwahab *et al.*, 2011 and Liu, 2009).

Al-Si-Mg alloys are usually subjected to T6 heat treatment that consist solution heat treatment and artificial ageing. The solution treatment at 540^0C - 550^0C would result in dissolution of the hardening phase (Mg_2Si) in the matrix, the homogenization of the cast alloy and the spheroidization of the brittle silicon (Shuhui, 2006). After solution treatment the alloy is then aged at low temperatures ranging from 150^0C to 200^0C for precipitation of the hardening compounds to improve the mechanical properties of the matrix.

The heat treatment of aluminum alloys improves their hardness, tensile strength, and electrical conductivity, making the alloys more suitable for the manufacture of aircraft and automobile components. Magnesium addition makes Al-Si alloy heat treatable (Zou *et al.*, 2010) and hence improves its mechanical properties by forming Mg_2Si phase (Kuntongkun *et al.*, 2008), while silicon improves fluidity and reduce solidification shrinkage thus improving castability. Antimony addition into Al-Si alloy has been proven to refine the eutectic silicon in the alloy, and also caused an increase in the mechanical properties of A356 by reducing secondary dendrite arm spacing (SDAS) in castings (Boontein *et al.*, 2008).

Di Sabatino, (2005) studied the effect of different modifiers on the fluidity of eutectic Al-Si alloys, and observed that fluidity decreased with the additions of Na, (Na + Sr), Ti, (Na +Ti), (Na + Sr + Ti), but increased with the additions of Sb or (Sb + Ti). Comalco (1997), confirmed that Sb does not fade and is insensitive to regassing, making Sb a better modifier. Fluidity of molten metal is important, particularly, for the aerospace and automotive industries in order to realize thinner and lighter products (Di Sabatino *et al.*, 2005).

However, when an aluminum alloy such as Al-Si-Mg exhibits satisfactory mechanical properties under controlled laboratory tests, it is pertinent to conduct an investigation on its corrosion behavior (Escalera-Lozano *et al.*, 2010). It is well known that the corrosion behavior of aluminum alloys is significantly affected by the presence of particles such as Mg2Si, which tends to be anodic with respect to the matrix and act as initiation sites for pitting corrosion.

Al-Si -Mg alloys has a long history, and is still widely used in aeronautical, automobile and marine industries. However, very little work has been done on the effect of antimony and preaging on the hardness and corrosion behaviors of Al-Si-Mg alloy. In this work, comparative study of the effects of the various pre-aging heat treatment temperatures with tolerable amount of antimony addition to this alloy system on the hardness, corrosion behavior and microstructures have been investigated.

1.1 JUSTIFICATION OF THE RESEARCH

The extended use of Al-Si-Mg alloys such as A356 and A357 (modified 356 and 357) (www.alcotec.com, 2005), for aerospace, marine and automobile components, has motivated studies for improving the mechanical and corrosion performance of these alloys. However, major drawbacks are: cost, availability, and effectiveness of chemical alloying elements and choice of heat treatments. Al-Si-Mg alloys with 0.01wt% Sb was considered best by some researchers (Comalco, 1997), and pre-ageing being unavoidable before artificial ageing, are impetus to this study; to improve properties that can withstand corrosion, better hardness and reduce cost of maintenance and replacement of components built from these alloys.

1.2 AIMS AND OBJECTIVES OF THE RESEARCH

The aim of the research is to investigate the hardness, microstructure and corrosion characteristics of antimony modified Al-Si-Mg alloy in the as-cast, pre-aged and age-hardened conditions in artificial seawater environment. For the aim to be achieved, the following objectives were undertaken.

I. To produce Al-Si-Mg alloy and subject the alloy to variable pre-ageing treatments.

II. To investigate the hardness of the alloy in the as-cast and age-hardened conditions.

III. To carry out microstructural characterization of the alloy using Optical Microscope (OPM), X-ray Diffractometry and Scanning Electron Microscope (SEM).

IV. To investigate the corrosion characteristics of the alloys in simulated seawater environment.

V. To correlate the results obtain from hardness/Corrosion characteristics with microstructure of the alloys.

1.3 SCOPE OF WORK

The scope of the work covers; production of the alloy by chill casting method, pre-ageing of the alloy produced and artificial ageing, hardness testing, corrosion testing and evaluation of the microstructural morphology of the alloy. The hardness was investigated, because the intention of the alloy is to withstand the application in the service condition in the area of automobiles and structural industries.

The corrosion rate of the alloy was measured using linear polarisation and weight loss methods. The alloy was also tested in artificial seawater because of the Navy's unique requirement, as the alloy may be used in an aggressive conditions where it may often encounter salt water spray or salt fog or both and could also be applied in the oil and gas industries. Finally, the full microstructural characterization and identification of the phases in the alloys was carried out.

1.4 CONTRIBUTION TO KNOWLEDGE

1. Presently, to the best of my knowledge there is no previous work on antimony modified Al-Si-Mg alloy in which variable heat treatments conditions were investigated.
2. The hardness value and corrosion resistance of the STAT-T6 were improved as a result of varying the pre-ageing temperature and time of the Al-Si-Mg alloy studied

CHAPTER TWO

2.0 LITERATURE REVIEW

2.1 CLASSIFICATION AND DESIGNATION OF ALUMINUM ALLOYS

2.1.1 Classification

Aluminum alloys can be classified into two categories: wrought alloys and cast alloys. They can be further classified on the basis of their response to heat treatment. If they respond favourably to heat treatment, they are called 'heat treatable', which applies to both, cast and wrought alloys. Some alloys are not heat treated and used only in the cast condition. Wrought alloys are formed by rolling, forging and extrusion into useful products, whereas cast alloys are directly cast into finished products (Zaki, 2006). Aluminum alloys can also be categorized based on the particular materials characteristics such as its ability to respond to thermal and mechanical treatment and the primary alloying element added to the aluminum alloy. These characteristics are identified in the numbering / identification system used for aluminum alloys. The wrought and cast aluminums have different systems of identification (www.alcotec.com, 2005).

2.1.2 Designation of Aluminum Alloys

Aluminum Association and the American National Standard Institute use a four digit numerical system to identify aluminum alloys (Schweitzer, 2007). The system used for wrought alloys is slightly different from that used for cast alloys and both are described in Table 2.1 and Table 2.1 respectively. For wrought alloys the first digit indicates the alloy group and the last two digits identify the aluminum alloy or indicate the aluminum purity. The second digit indicates modifications of the original alloy or impurity limits. Experimental alloys are also identified in accordance with this system, but they are indicated as experimental by the prefix X. The first digit used for casting alloys and foundry ingots also identifies the alloy group. However, the second two digits identify the aluminum alloy or aluminum purity. The last digit, which is preceded by a

decimal point, indicates the product form (i.e., .0 for casting and .1 for ingot). A serial letter before the numerical designation indicates a modification of the original alloy or impurity limits. The X is reserved for experimental alloys (Blankenship *et al.*, 1992 and www.alcotec.com, 2005).

Table 2.1 Aluminum Alloy Designation Systems for Wrought Alloys (Blankenship *et al.*, 1992)

Wrought alloys	Four-digit designation
99.00% (min) aluminum	1XXX
Copper	2XXX
Manganese	3XXX
Silicon	4XXX
Magnesium	5XXX
Magnesium and silicon	6XXX
Zinc	7XXX
Others	8XXX

Tempers Designation System (www.aluminum.org, 2012)

F - As-fabricated

O - Annealed

H - Strain-hardened (wrought products only)

W- Solution heat-treated

T - Thermally treated to produce tempers other than F, O, H (usually solution heat-treated, quenched and precipitation hardened)

Numeric additions indicate specific variations e.g.

T6 - solution heat treated and artificially aged

2.1.2.1 Cast Aluminum

Table 2.2 Aluminum Alloy Designation Systems for Casting Alloys (Blankenship *et al.*, 1992 and Apelian, 2009)

Number Series	Alloy Type
1XX.X	99.0%minimum aluminum content
2XX.X	Al + Cu
3XX.X	Al + Si & Mg, or Al + Si & Cu, or Al + Si & Mg & Cu
4XX.X	Al + Si
5XX.X	Al + Mg
7XX.X	Al + Zn
8XX.X	Al + Sn

In the North America Die Casting Association (NADCA) numbering system, major alloying elements and certain combinations of elements are indicated by specific number series, as follows: The digit that follows the decimal in each alloy number indicates the product form. A zero (0) following the decimal indicates the cast product itself (die casting, for instance). A one (1) following the decimal indicates the chemistry limits for ingot used to make the XXX.0 product. A two (2) following the decimal also indicates ingot used to make that XXX.0 product, but ingot of somewhat different (usually tighter) chemistry limits than that of XXX.1. While not always the case, XXX.1 often indicates secondary alloy chemistry limits whereas XXX.2 would indicate primary alloy chemistry limits. For example, a designation 380.0 could indicate a die cast product likely produced from 380.1 secondary ingots whereas 356.0 might indicate a squeeze cast product produced from 356.2 primary ingots. The important things to remember are that a "0" following the decimal indicates a cast product whereas a "1" or "2" indicates the ingot chemistry needed to make the cast product. Since melting and melt handling can alter the chemistry of an alloy prepared to make castings, the "XXX.1" or "XXX.2" ingot specifications are always somewhat tighter than the "XXX.0" specifications for the cast part. And according to convention, "XXX.2" ingot always has tighter chemistry limits than "XXX.1" ingot (Apelian, 2009).

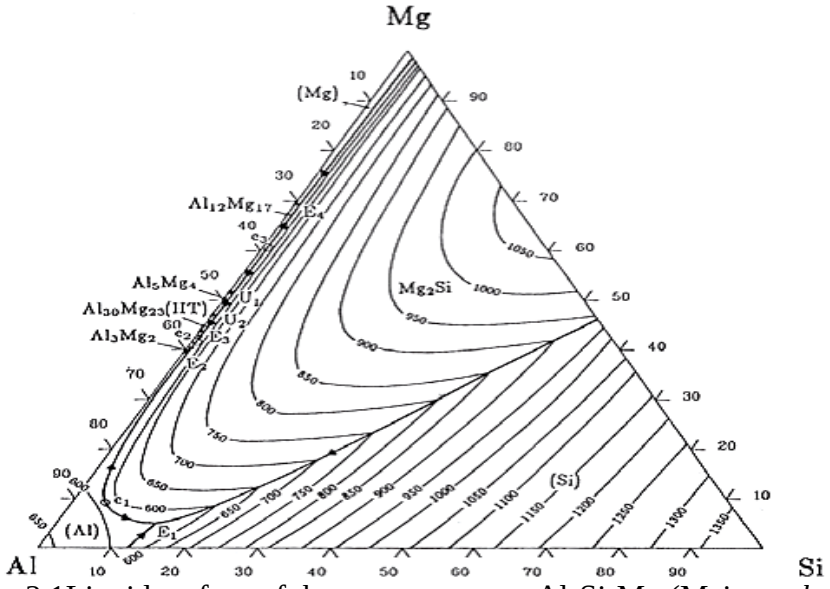


Figure 2.1Liquid surface of the ternary system Al-Si-Mg (Maja *et al.*, 2006)

2.2 Ternary phase diagram of Al-Si-Mg alloy

Ternary phase diagrams represent the equilibrium between three components, as a function of temperature. The concentration of each of the three components can be express as either weight percent or molar percent. The sum of the three components must add up to 100 percent. The overall compositions of the components are usually determined using Gibbs triangle, which is an equilateral triangle on which the pure compounds are represented by each corners (Figure 2.1 and 2.2).

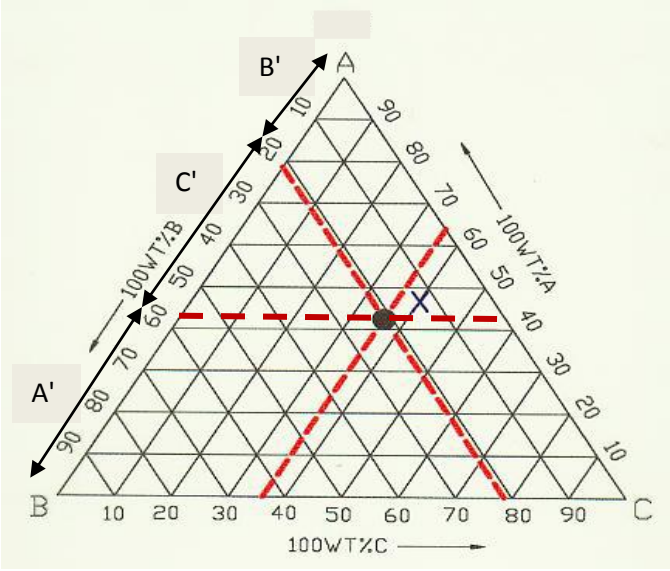


Figure 2.2 Ternary Phase diagram for a composition base for an ABC (Selvaduray, 2004).

Determination of the overall composition of alloy X for instance (Figure 2.2), involves drawing lines to pass through X, and parallel to each of the sides. Where distance A' gives the concentration of component A in X, B', the concentration of B and C' the concentration of C in X respectively (Selvaduray, 2004).

2.3 Heat-treatable aluminum alloy

Precipitation hardening is a heat treatment process that harnesses the ability of precipitated nanoscale and microscale intermetallic impurities to impede the creation and propagation of lattice defects, such as dislocations. By doing so, these precipitates greatly strengthen the metal matrix (www.about.com.metals). Controlled heat treatment of aluminum alloys can significantly influence properties such as strength, ductility, fracture toughness, thermal stability, residual stresses, dimensional stability, and resistance to corrosion and stress corrosion cracking. The main heat treatment procedures are homogenization, annealing, and precipitation hardening involving solution heat treatment, quenching, and ageing heat treatment (Jacobs, 1999). A temper designation system has been developed by the Aluminum Association to describe the processing of wrought and cast aluminum alloys (Table 2.1 and 2.2).

2.4 Precipitation Hardening Heat Treatment

Precipitation treatment or age hardening is one of the most widely used heat treatment for the strengthening of metal alloy (Durmus and Meric, 2007). Some precipitation treatments purposely overage the alloy beyond the maximum strength condition (T6 temper-Solution Heat Treated and Artificially Aged) (MHB, 1990) to improve its resistance to intergranular corrosion (IGC), exfoliation, and stress corrosion cracking (SCC) through the formation of randomly distributed, noncoherent precipitates (T7 tempers-solution heat treated and overaged or stabilized) (Roberge, 1999).

Precipitation hardening involves raising the temperature of the alloy into the single phase region so that all of the precipitates dissolve. The alloy is then rapidly quenched to form a supersaturated

solid solution and to trap excess vacancies and dislocation loops which can later act as nucleation sites for precipitation. The precipitates can form slowly at room temperature (natural aging) and more quickly at slightly elevated temperatures, typically 100°C to 200°C (artificial aging). The degree of hardening obtained depends on the size, number and relative strength of the precipitates. These factors are determined by the composition of the alloy, tempering temperature and tempering time (ASM, 1984).

Differences in type, volume fraction, size, and distribution of the precipitated particles in an alloy microstructure, govern the properties as well as the changes observed with time and temperature, and these are all affected by the initial state of the structure. These conditions, the time and temperature of precipitation heat treatment, affect the final structure and the resulting mechanical properties of an alloy.

Alloys in T6-type tempers generally have the highest strengths without sacrificing minimum levels of other properties and characteristics making the alloy suitable for engineering applications. Alloys in T7 tempers are overaged, which means that some degree of strength has been sacrificed or "traded off" to improve one or more other characteristics (Key to Metals, 2010).

2.4.1 Solution Heat Treatment

Solution heat treatment is carried out to homogenize the alloy. It involves heating an alloy at a high temperature for a specific period of time, and then rapidly cooling or quenching in water or a water-glycol solution (Avcorp, 2012). During solution treatment, the alloy is subjected to high temperatures for relatively long periods of time with two main objectives (Tavitas-Medrano *et al.*, 2008):

i. To obtain maximum solubility and homogeneity of the alloying elements in the matrix.
ii. To modify the acicular morphology of the eutectic Si to a less detrimental rounded one.

The solution temperature should be high enough and the treatment time long enough to obtain maximum solubility and homogeneity of the alloying elements. However, control of the solution

treatment temperature and time is very important because, if the melting point is exceeded, localized melting at the grain boundaries would occurred and the mechanical properties reduced, while increasing the solution time may result in the coarsening of the structure (Kezhun *et al.*, 2011). Solution heat treatment is employed to achieve maximum concentration of solute in solid solution. The temperature is determined based on the composition and maximum solid solubility, and is normally achieved by heat treating near, but below, the eutectic temperature. Solution heat treatment time depends on microstructure, section thickness, and furnace loading and can vary from less than a minute to 20 hours. A short solution treatment of 30 minutes at 540 or 550°C is sufficient to achieve almost the same mechanical property level as that with a solution treatment time of 6 hrs (Peng *et al.*, 2011). Aluminum-silicon casting alloys, in which the eutectic silicon is modified by the addition of elements such as strontium, sodium, or antimony, undergo rapid spheroidization of the silicon particles, while complete spheroidization is never achieved in unmodified alloys (Erhard, 2002 and Moller *et al.*, 2008).

2.4.2 Precipitation Hardening

Phase transformations in alloys can generate particles or "precipitates" of a second phase, which may differ from the matrix by their composition or their structure (whether crystalline or amorphous). Important parameters of precipitation-hardened alloys are the strength of the precipitate phase, its volume fraction, and the dispersion of the particles – their mean size and the typical distance between them (Ernst, 2004).

Precipitations hardening process begins with a solution heat-treatment i.e. all alloying elements are in solid solution; follow by quenching to obtain a uniform distribution of all elements at ambient temperature. After that the elements involved begin to diffuse in the aluminium matrix, they unify to intermetallic compounds and grow. This happens at room temperature but with more efficiency at elevated temperatures (natural ageing and artificial ageing). It is important to know that the hardening effects due to precipitations can also decrease if too high temperatures are acting for a short time on the material or more moderate temperatures for a longer period (Gitter,

2008). Variations in thermal treatments can have marked effects on the local chemistry and the local corrosion resistance of high-strength, heat-treatable aluminum alloys (Roberge, 1999).

During natural aging of Al-Si-Mg alloys, hardening is believed to occur due to the precipitation of solute clusters and Guinier-Preston (GP) zones but during artificial aging, these clusters and GP zones transform to the strengthening β" phase (needles), followed by β' (rods). These phases are the precursors of the equilibrium β phase (plates). In summary, considering the Al-Si-Mg phase diagram (Figure 2.1), decomposition of the supersaturated solid solution (SSS) of these alloys (containing an excess of Si) occur in the following way (Liu, 2009; Ernst, 2004):

SSS→ GP (I) $_{\text{spherical}}$ → GP (II) β" $_{\text{needles}}$ → β' $_{\text{rods}}$ → β (Mg_2Si) platelet (Abdulwahab *et al.*, 2011)

Where

GP - Guinier-Preston Zones

β- Equilibrium Mg_2Si

β' and β"- Metastable precursors of β

In practice, it is difficult for artificial aging to be performed immediately after solution heat treatment since a delay at room temperature (i.e. low temperature aging treatments or preaging) prior to thermal aging is usually unavoidable (Zhen and Kang, 1997 ; Hirth *et al.*, 2001).

2.5 THE EFFECT OF ALLOYING ELEMENT ON THE MECHANICAL PROPERTIES, MICROSTRUCTURES AND AGE-HARDENING RESPONSE OF ALUMINUM ALLOYS

Pure aluminium serves no purposeful industrial applications due to its poor mechanical properties. However, various elements are added to pure aluminium to enhance tensile strength, hardness (Omotoyinbo and Oladele, 2010), ductility or any other mechanical characteristic. Mechanical properties are usually enhanced by alloying additions and heat treatments. Some chemical elements are added to pure aluminium to provide different results. The principal and most

effective elements are Silicon, Copper, Magnesium, Iron and Zinc (Andreatta *et al.*, 2004). Though, Si is always present in the principal commercial alloys, but the effects of major alloying elements are as follows: silicon, improve fluidity and reduce solidification shrinkage thus improving castability of silicon based aluminium alloys. It also increases strength until the eutectic level percentage is reached. Copper and Mg strengthen the alloy matrix, improve the mechanical properties and machinability (Tash *et al.*, 2007 and Tash *et al.*, 2008) also, promote strengthening through forming the precipitation hardening phases such as Al_2Cu, Mg_2Si and Al_2CuMg (Caia *et al.*, 2011). Zinc enhances maximum mechanical properties of aluminium alloys in the as-cast condition. Iron as an element is always present in Al-Si alloys as a carryover of the alloy processing and handling. In concentrations above 0.7wt percent iron has detrimental effects to mechanical properties but, manganese is often used to counter its effects (Kosgey *et al.*, 2011).

Abdulwahab *et al.*,(2012) study on A356.0 alloy, investigated the effect of different tempers and thermal ageing treatments on the hardness characteristics and yield strength of A356.0 alloy. Their investigations involve artificial ageing without solution heat treatments (T5), solution heat treated with artificial ageing (T6), interrupted-quenching-ageing (IQA) and step-quenching-ageing (SQA) under artificial ageing condition. They observed that, the SQA treated alloy improved the hardness. However, that the ageing temperatures and time considered at various conditions, favoured the strengthening phases that contributed to the higher hardness of the samples.

Hassan and Aigbodion, (2009) studied the microstructure and ageing behavior of Al-Si-Fe alloy with varied additions of Mg i.e. 4.0-6.0wt% and observed that there were increases in hardness values and strength during ageing of the alloy, which was attributed to the formation of coherent and uniform precipitation in the metal lattice. More so, that addition of 5.0wt% Mg to the alloy accelerates its thermal ageing treatment, indicating that better mechanical properties was achieved when the as-cast Al-Si-Fe/Mg alloy was subjected to thermal ageing treatment.

Mg_2Si. Masuda *et al.*, (2010) worked on combined effect of pre-straining and pre-aging bake-hardening behaviour of Al-0.6Mg-0.1Si and observed that dislocations induced by pre-straining

reduce the concentration of quenched-in excess vacancies, resulting in both suppressed clustering of solute atoms during pre-aging and the accelerated precipitation of the β" phase from more supersaturated solute atoms in final ageing.

2.5.1 Eutectic Modification of Al-Si-Mg alloys

Modification is the change in scale and morphology of the eutectic Si from a coarse flake-like structure to a fibrous or fine flake structure in Al-Si-Mg alloys. It is important to modify the eutectic Al-Si-Mg alloys to improve strength, ductility, pressure tightness and machinability (Al – Helal, 2013). Modifiers such as antimony, calcium, sodium and strontium are added to eutectic or hypoeutectic aluminum silicon magnesium casting alloys to modify the morphology and microstructure of the eutectic silicon phase. Eutectic silicon if not modified, solidifies in a relatively coarse continuous network of thin platelets, providing abundant stress risers and thus limits to achieve maximum strength and ductility. Modification with one of Sb, Ca, Na and Sr can change the eutectic silicon into a fine fibrous or lamellar structure leading to good mechanical properties (Rana *et al.,* 2012).

Hong *et al.*, (2010) investigated the influence of Sb on the microstructure and mechanical properties of Mg2Si/AM60 composite and their result indicated that there was a formation of Mg_3Sb_2 particles due to the addition of Sb. The Mg_3Sb_2 promoted the formation of polygonal type Mg_2Si with the provision nucleation site. Their result also shows that the grain size of Sb modified alloy was finer than that of the matrix. The improved microstructure, improved the mechanical properties. The addition of Sb up to 0.8% increased the ultimate tensile strength by 12.2%. Also observed, was formation of new phase with addition of Sb which provides nucleation core of

2.6 CORROSION PROPERTIES OF ALUMINUM AND ITS ALLOYS

The corrosion resistance of aluminium and its alloys is largely due to the protective oxide film (Nestor, 2004) which within seconds attains a thickness of about 1.0nm (Fontana and Greene, 1987) on freshly exposed metals; continuation of growth is markedly influenced by the environment, being accelerated by increasing temperature and humidity. This film is resistant to

attack from water and oxygen in a wide range of temperatures and pH levels, making aluminum alloys useful in a variety of environments (Escalera-Lozano *et al.*, 2010). Immersion in water results in rapid oxide thickening. However, the presence of aggressive ions like chloride creates extensive localized attack (Fontana and Greene, 1987). The behaviour of the oxide may be modified by impurities or alloying additions. The possible effects of minor impurities or additions is well illustrated in the case of tin, whose modifying effect upon the oxide is utilized in obtaining a highly electronegative potential in aluminium sacrificial anodes.

Alloying element additions to aluminum change the electrochemical potential of the alloy, which affects corrosion resistance even when the elements are in solid solution. Zinc and magnesium tend to shift the potential markedly in the anodic direction, whereas silicon has a minor anodic effect. Copper additions cause marked cathodic shifts, that result to local anodic and cathodic sites in the metal which affect the type and rate of corrosion (Roberge, 1999).

The oxidation of aluminium at room temperature is reported to conform to an inverse logarithmic equation for growth periods up to 5 years duration. At elevated temperatures, oxidation studies over shorter periods illustrate conformity to parabolic, linear and logarithmic relationships according to time and temperature. These kinetic variations are attributed to different mechanisms of film formation.

Osorio *et al.*,(2007) investigated the influence of Al_2Cu intermetallic particles associated to the dendritic arm spacing on the general corrosion resistance, by considering three different hypoeutectic Al-Cu alloy samples in a 0.5M H_2SO_4 at 25^0C.They observed that Al_2Cu has a less noble corrosion potential than the Al-rich phase. Hence the dendrite fineness had more influence on corrosion resistance than the increase on alloy copper content with consequence increase on Al_2Cu fraction.

Jaukovic and Asanovic,(2006) investigated the effect of temper and chemical composition on polarization resistance of aluminum RR58 alloy and observed that plastic deformation had a significant influence on corrosion behavior of the alloy. Consequently, the addition of Zr above

0.18% and Lanthanides contributed to the corrosion resistance of the alloy after precipitation heat treatment.

Reda *et al.*,(2008) studied the improvements in mechanical and stress corrosion cracking properties of Al-alloy7075 via retrogression and reaging. They observed that preaging atT6 120^0C and retrogression at T7 200^0C resulted in the highest hardness and tensile properties of the alloy. The preaging and retrogressing at the same conditions led to the deterioration of corrosion properties of the alloy. They equally stated that the coarse precipitates found during retrogression and reaging after seven days of immersion in 3.5% NaCl solution became a hydrogen trapping sites.

Li *et al*,(2008) compared different heat treatments such as T6, RRA (retrogression and reaging), T616, T73 and HTPP (high temperature pre precipitation) to improve the corrosion resistance of 7075 aluminum alloy. They observed that T6, RRA and T616 improved the alloy intergranular and exfoliation corrosion resistance while the alloy still maintained its high strength. However, T73 and HTPP (high temperature pre-precipitation) thus improved the corrosion resistance of the alloy but lowered its strength.

Andreatta *et al.*,(2004) investigated the corrosion behavior of different tempers of AA7075 aluminum alloy. They reported that the alloy is susceptible to localized corrosion, such as pitting, intergranular and exfoliation corrosion. More so, that the localized corrosion of the alloy initiates at the Cu- and Fe-rich intermetallics due to the presence of high Volta potential difference between the intermetallics and the matrix. Furthermore, that the Volta potential differences increases when the alloy was solution heat treated, but decreases when aged to the peak strength T6 temper and to the T7 temper.

Abdulwahab *et al.*,(2011) studied the effect of multiple-step thermal ageing treatment (MSTAT) on the corrosion characteristics of A356.0-type Al-Si-Mg alloy in simulated seawater. They observed the corrosion effects under double thermal ageing (DTAT-T7), single thermal ageing (STAT-T6) and step quenching and ageing (SQA) and hence reported that, the alloy suffers

uniform corrosion which was predominantly a pitting corrosion, and that the pits diameter ranged between 30-50μm.

2.7 APPLICATIONS OF ALUMINUM BASED ALLOYS

Structural: Aluminum alloys are used extensively for structural and architectural applications. Their corrosion resistance, light weight and high strength are advantageous in aerospace (leading and trailing edges, access covers, seat tracks and wing skins), automotive parts (oil pan, rear-axle housing, crank cases, engine blocks, airframes, cylinder head, propellers, accessories, as tank for storage of liquid fuels and oxidizers), and marine applications.

Foods, Pharmaceuticals, and Chemicals: Aluminum and aluminum base alloys are widely used in the processing, handling, and packaging of foods, beverages, and pharmaceutical and chemical products based on their economic factors and the excellent compatibility with many of these products (Davis, 2000 and Apelian, 2009).

CHAPTER THREE

3.0 MATERIALS AND METHODS

3.1 MATERIALS

The material used in this research include; high purity aluminium wire, pure silicon powder (Si), Magnesium chips (Mg), antimony powder (Sb), etchants (Keller's reagent), distilled water, sodium chloride granules, ethanol, measuring cylinder and thread.

3.1.1 Equipment

The following equipment were used, Muffle electrical resistance furnace (for the heat treatment), Labotec water heater (CPH 110) (used to heat water for quenching), plastic containers, polishing machine, split cylindrical steel moulds, moulding boxes, Indentec Hardness Testing machine (model: 818.5LKV), Metallurgical Optical Microscope (NJF-120A), Digital Weighing balance (Setra-BL410S), XRD, Electrochemical potentiostat corrosion kit: Autolab-GPES (model: AuT71791 and PGSTAT30), SEM-EDS (Joel: JSM-7500F)

3.2 METHODS

3.2.1 Casting of the Samples

The Al-Si-Mg alloys with chemical composition shown in Table 3.1 were melted using a muffle resistance furnace that was allowed to heat to 750^0C, the crucible was removed and other alloying elements added. The crucible was then returned to the furnace to heat for 30minutes during which the temperature of the melt was raised to 800^0C, and then Mg was added to the melt in the ladle before pouring into the mould. The cast samples were machined to 20mm diameter by 30mm length dimensions for hardness and corrosion tests.

Table 3.1: Chemical Composition of the produced Al-Si-Mg Alloy (wt %)

Al	Si	Mg	Mn	Cu	Fe	Ti	Zn	Sb
92.92	6.5	0.35	0.03	0.03	0.08	0.05	0.03	0.01

Table 3.2: Summary of Sample Number, Analysis and Properties for Al-Si-Mg Alloy Studied.

Analysis/ Properties	Hardness	Corrosion		Microstructural Study	XRD Spectrum	Total
		Weight loss	Electrochemical			
Sample Number	17	340	17	4	2	380

3.2.1 Heat Treatment

As shown in Table 3.2, a total of three hundred and eighty (380) machined samples were used for hardness test, corrosion test, XRD, OPM and SEM; three hundred and fifty four (354) samples were solution heat treated at temperature of 540^0C for 1hr in an electrical furnace and then rapidly quenched in warm water. The quenched samples were given STAT and DTAT ageing treatments as described below.

3.2.1.1 Single Thermal Ageing Treatment (STAT-T6)

A total of twenty two (22) samples were solution treated at 540^0C for 1hour, quenched in warm water (65^0C), artificially aged at 180^0C for 2hours and finally cooled in air.

3.2.1.2 Double Thermal Ageing Treatment (DTAT-T7)

A total of three hundred and thirty two (332) samples were given a double thermal ageing treatment consisting of solution heat treatment at 540^0C for 1hour, quenching in warm water (65^0C), pre-ageing at temperatures 90^0C, 105^0C and 120^0C for 1-5hours, artificial ageing at 180^0C for 2hours and finally cooled in air.

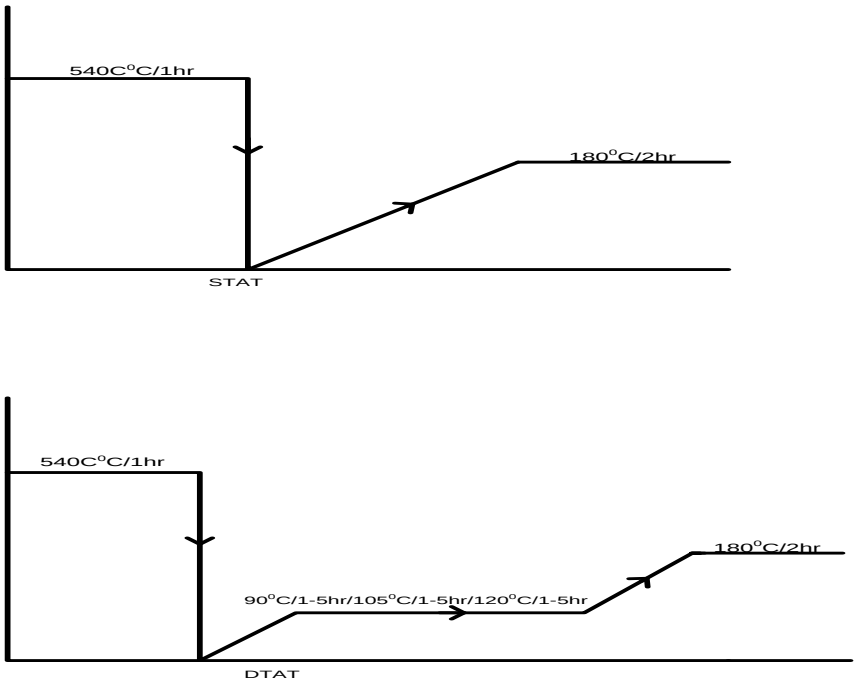


Figure 3.1 Schematic diagrams of STAT and DTAT heat treatment cycles used

3.2.2 Hardness Measurement

Hardness test were carried on a total of seventeen (17) samples comprising of As-cast, STAT and DTAT samples. The anvil of the Rockwell hardness-F scale tester was properly cleaned before samples of 20mm diameter x 30mm thickness in dimensions were each placed and well supported to prevent any movement during the test, since any slight movement can significantly alter the hardness results as it can be reflected as an error in the depth measurement.

The hand wheel was smoothly rotated clockwise to uplift the anvil until the sample has been contacted with indenter. The hand wheel is further rotated slowly and smoothly until the cursor reaches the end position, where a buzzing warning was given out indicating that the rotation should be stopped at once and the hardness value at each state was obtained by an average of three measurements.

3.2.3 X-Ray Diffractometry (XRD) Measurement

XRD measurement was carried out on two (2) samples (as-cast and DTAT with the highest hardness value). The As-cast and the thermally treated samples were milled into 20mg powder, collected in plastic tray and placed in the XRD machine while, the acquisition system attached to the machine displayed the samples phase properties.

3.2.4 Corrosion Characteristics

3.2.4.1 Weight loss technique

The weight loss technique was used to characterize the corrosion rate of three hundred and forty (340) samples comprising of As-cast, STAT and DTAT samples. Sets of same concentration of 3.5w% NaCl in 100ml were prepared (for the As-cast and heat treated). The coupons were cleaned before being suspended in the NaCl solutions with the aid of threads.

Weight losses of the coupons were taken at intervals of two days (48hr) over a period of forty days (960hr). After removing the coupons from the solution, the surfaces were then scrubbed with brush in distilled water, rinsed in ethanol and air dried before weighing.

3.2.4.2 Electrochemical Potentiodynamics technique

A total of seventeen (17) samples which comprised of As-cast, STAT and DTAT samples were subjected to electrochemical potentiodynamics technique to characterize the corrosion rate (current density), which consists of cyclic scan. A potentiostat coupled to a computer system, a glass corrosion cell kit with graphite rods as counter electrodes and a saturated Ag/Ag reference electrode were used. The working electrodes consist of the thermally treated samples. The samples were positioned at the glass corrosion cell kit, leaving a 3.808 cm^2 alloy surfaces in contact with the solution. Polarization test were carried out in a 3.5wt% NaCl solution at room temperature in a static solution for a period of 30 minutes each using a potentiostat. The polarization curves were determined by stepping the potential at a scan rate of 0.0016V/sec. The

polarization curves were plotted using Autolab data acquisition system (Autolab model: Aut71791 and PGSTAT 30), and both corrosion rate and potential were estimated by the Tafel extrapolation method (corrosion rate analysis) using the anodic and cathodic branches of the polarization curves.

3.2.3 Corrosion Rate Measuring Technique

The weight loss (W) is determined as the differences between the initial weight (Wo) of the coupon and the final weight (Wf) after forty eight hours interval:

$$W = Wo - Wf \qquad \text{Equation (3.1)}$$

The corrosion rate will be determined in millimetre per year (mm/yr) using relationship (Fontana and Greene, 1987; Callister, 2001)

$$Corrosion\ penetration\ rate(mm/yr) = \frac{\mathrm{KW}}{\rho At} \qquad \text{Equation (3.2)}$$

Where:

K = Constant = 82.8 mm/year

W = Weight loss (mg)

Wo = Initial weight of coupon

Wf = Final weight of coupon

ρ = Density of the material, g/cm^3

t = Exposure time, hrs

A = Cross – sectional area, cm^2

3.4.5 Microstructural Examination

The four (4) samples for microscopic examination were machined out from the cylindrical castings. The samples were ground with emery papers of progressively fine grade 80, 220, 400 and 600 grits. The samples were turned through 90° between papers and washed thoroughly with water before proceeding from one paper to the next. Final polishing was performed in rotating discs of proprietary cloth charged with diamond paste of 6μm particle size. Then the samples were washed thoroughly with water and dried, followed by etching in Keller's reagent (95ml - H_2O, 2.5ml - HNO_3, 1.5 - HCl, 1ml - HF acid).The Optical microscope (OPM) and Scanning electron microscope (SEM) were used for the microstructure observations. The OPM were done in the Department of Metallurgical and Materials Engineering, Ahmadu Bello University Zaria, Nigeria and the SEM examinations were done at the Centre for Scientific and Industrial Research (CSIR) Pretoria, Republic of South Africa. The samples were held into the SEM microscopic region using the sample holder and allowed to remain stable for 30 seconds, after which the microstructure of the samples were displayed upon adjustment of the magnification.

CHAPTER FOUR

4.0 RESULTS AND DATA PRESENTATION

The results of average hardness measurement (HRF), corrosion rate analyses from the weight loss and the linear polarization using the data from the Tafel plots on As-cast, STAT and DTAT samples are presented in Tables 4.1 – 4.7

Table 4.1: Average HRF-F scale value measurement

	Average HRF Value				
Pre-ageing time(hr)	**As-Cast**	**180^0C/2hr**	**90^0C+180^0C/2hr**	**105^0C+180^0C/2hr**	**120^0C+180^0C/2hr**
	5.03	6.13	-	-	-
1	-	-	7.80	6.90	7.70
2	-	-	8.40	6.83	6.73
3	-	-	7.27	7.63	6.47
4	-	-	7.28	6.27	5.83
5	-	-	7.60	7.27	5.77

Table 4.2: Linear polarization data of thermally pre-aged Al-Si-Mg alloy at 90^{o}C in 3.5%NaCl solution at 25^{0}C.

Samples	**ba (V/dec)**	**bc (V/dec)**	**Ecorr, Calc (V)**	**Ecorr, Obs (V)**	**jcorr (A/cm²)**	**icorr (A)**	**Corrosion rate (mm/year)**	**Polarization resistance (Ω)**	**E Begin (V)**	**E End (V)**
As-cast	1.80840	0.40934	-2.02620	-0.73738	2.03E-03	7.72E-03	2.2814E+01	1.8780E+01	-1.38520	-0.02045
180/2hr	0.90993	0.37006	-1.70810	-0.73738	4.18E-04	1.59E-03	4.6947	7.1929E+01	-1.38520	-0.29388
90/1hr	2.50810	2.66340	-0.03033	-0.00543	2.67E-09	1.02E-08	3.00E-05	5.52E+07	-1.33640	1.33450
90/2hr	0.49673	0.60000	-0.79423	-0.28088	3.62E-06	1.38E-05	4.069E-02	8.5725E+03	-1.29490	0.28229
90/3hr	1.34900	1.16790	-0.81255	-0.26020	1.94E-05	7.36E-05	2.175E-01	3.6944E+03	-0.76263	0.65094
90/4hr	0.26755	0.35215	-1.3196	-0.73738	3.09E-05	1.17E-04	3.471E-01	5.6233E+02	-1.45840	-0.47699
90/5hr	0.62457	1.32600	-1.7963	-0.73738	6.28E-05	2.39E-04	7.056E-01	772.37	-1.11910	-0.34027

Table 4.3: Linear polarization data of thermally pre-aged Al-Si-Mg alloy at 105^{o}C in 3.5%NaCl solution at 25^{0}C.

Samples	**ba (V/dec)**	**bc (V/dec)**	**Ecorr, Calc (V)**	**Ecorr, Obs (V)**	**jcorr (A/cm^2)**	**icorr (A)**	**Corrosion rate (mm/year)**	**Polarization resistance (Ω)**	**E Begin (V)**	**E End (V)**
As-cast	1.80840	0.40934	-2.02620	-0.73738	2.03E-03	7.72E-03	2.2814E+01	1.8780E+01	-1.38520	-0.02045
180/2hr	0.90993	0.37006	-1.70810	-0.73738	4.18E-04	1.59E-03	4.6947	7.1929E+01	-1.38520	-0.29388
105/1hr	1.97240	0.39098	-0.51349	-0.25681	1.13E-09	4.29E-09	4.36E-06	3.30E+07	-0.41351	0.68024
105/2hr	0.13655	0.10418	-0.84398	-0.58038	4.68E-07	1.78E-06	5.265E-03	1.4409E+04	-1.05560	-0.48676
105/3hr	0.69848	0.15212	-1.03090	-0.80575	7.56E-06	2.87E-05	8.496E-02	1.8871E+03	-1.18500	-0.59662
105/4hr	0.22329	0.20785	-1.07380	-0.69286	9.69E-06	3.69E-05	1.089E-01	1.2686E+03	-1.31200	-0.50629
105/5hr	0.50142	0.27203	-1.18200	-0.58038	9.76E-05	3.71E-04	1.0971	2.0633E+02	-1.23870	-0.24750

Table 4.4: Linear polarization data of thermally pre-aged Al-Si-Mg alloy at 120^{o}C in 3.5%NaCl solution at25^{0}C.

Samples	ba (V/dec)	bc (V/dec)	Ecorr, Calc (V)	Ecorr, Obs (V)	jcorr (A/cm²)	icorr (A)	Corrosion rate (mm/year)	Polarization resistance (Ω)	E Begin (V)	E End (V)
As-cast	1.80840	0.40934	-2.02620	-0.73738	2.03E-03	7.72E-03	2.2814E+01	1.8780E+01	-1.38520	-0.02045
180/2hr	0.90993	0.37006	-1.70810	-0.73738	4.18E-04	1.59E-03	4.6947	7.1929E+01	-1.38520	-0.29388
120/1hr	0.02652	0.02847	-1.13480	-1.13890	6.09E-07	2.31E-06	6.84E-03	2.5766E+03	-1.15570	-1.10200
120/2hr	0.42163	1.19430	-0.72378	-0.19703	5.18E-06	1.97E-05	5.825E-02	6.8675E+03	-1.25820	0.65094
120/3hr	0.70032	1.21070	-1.05250	-0.16235	1.37E-05	5.23E-05	1.545E-01	3.6871E+03	-1.37540	0.99762
120/4hr	1.85630	1.27490	-1.88550	-0.20080	6.34E-05	2.41E-04	7.131E-01	1.3604E+03	-1.28510	0.49469
120/5hr	0.30584	0.26708	-0.87149	-0.73246	1.53E-04	5.8E-04	1.7142	1.0676E+02	-1.11910	-0.48676

Figures 4.1-4.7 show the curves for variation of hardness with ageing time of Al-Si-Mg alloy after Preaging at 90^0C, 105^0C, 120^0C; variation of Corrosion rate with ageing time for As-cast, STAT and DTAT of Al-Si-Mg Alloy at 90^0C, 105^0C, 120^0C from the weight loss in simulated seawater environment and linear polarisation of thermally pre-aged Al-Si-Mg alloy at 90^0C, 105^0C, 120^0C in 3.5% NaCl solution at 25^0C.

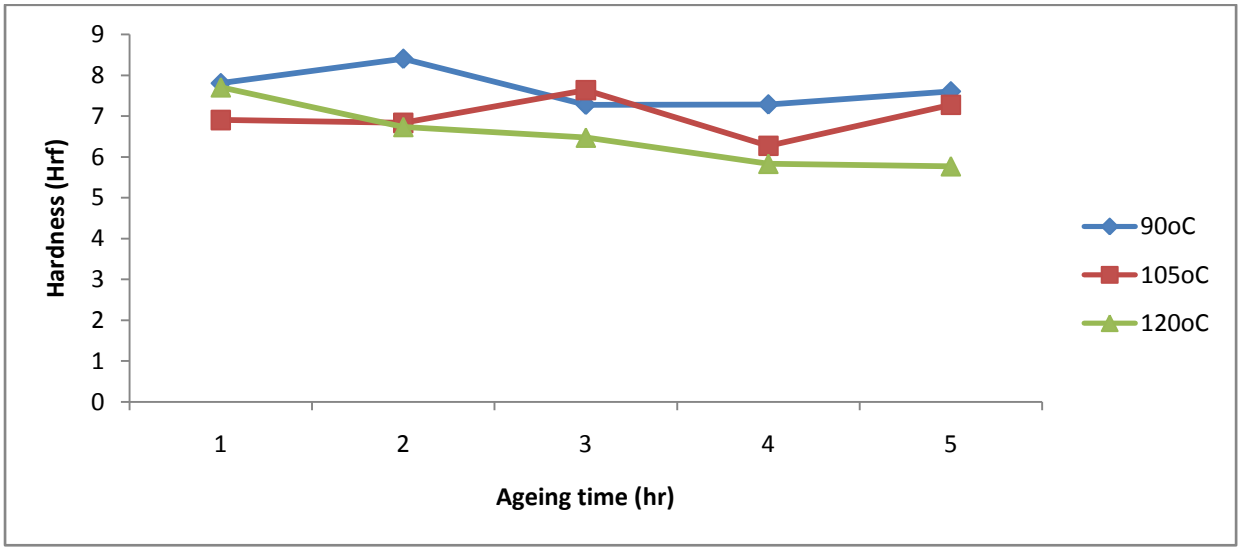


Figure 4.1: Variation of hardness with ageing time of Al-Si-Mg alloy after Preaging at 90^0C ,105^0C and 120^0C

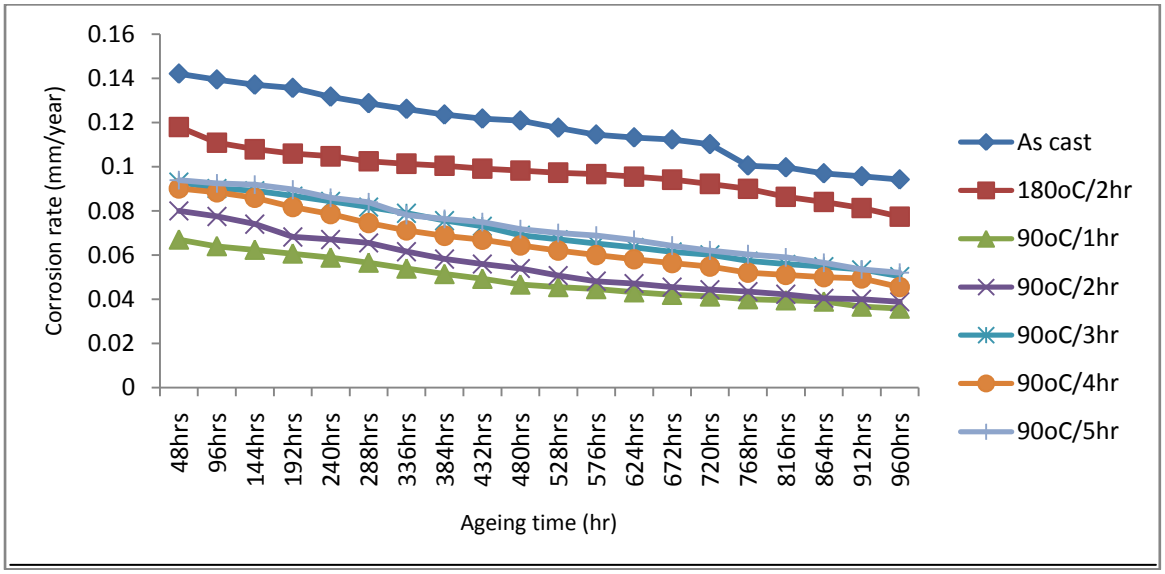


Figure 4.2: Variation of Corrosion rate with ageing time for As-cast, STAT-T6 and DTAT-T7 A356.0-Type Al-Si-Mg Alloy at 90^0C from the weight loss plot Data in Simulated Seawater Environment

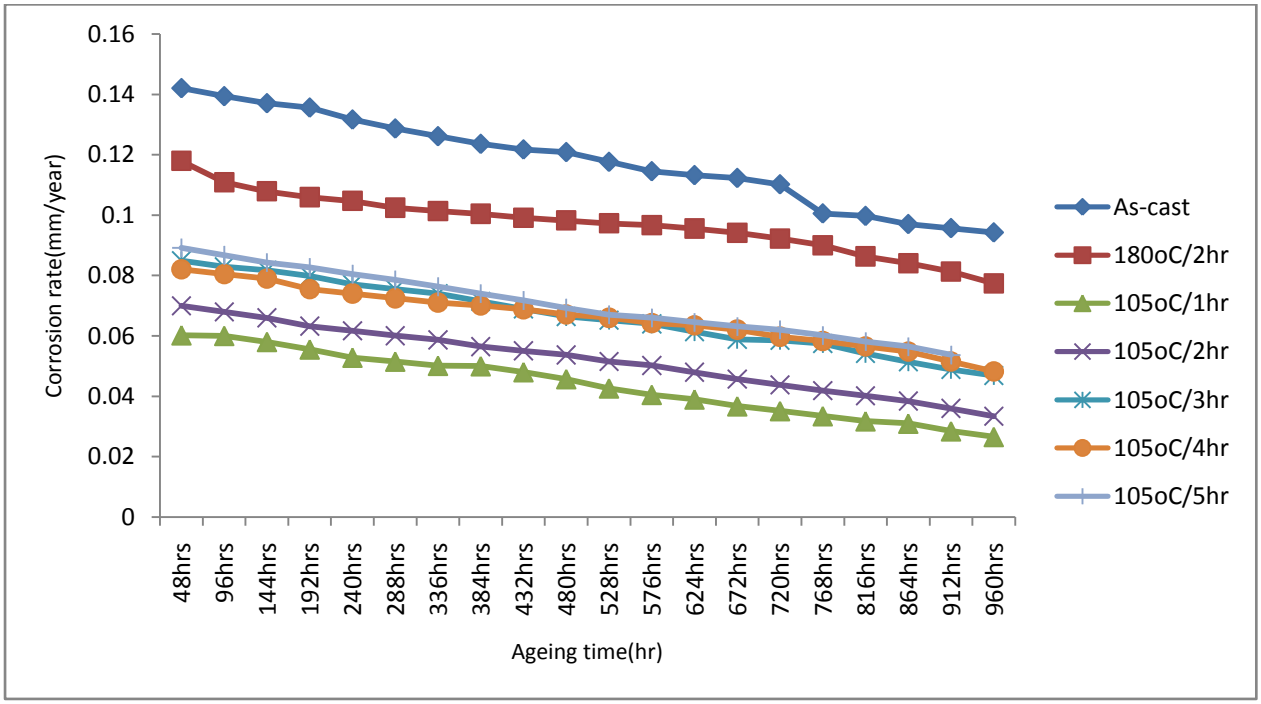


Figure 4.3: Variation of Corrosion rate with ageing time for As-cast, STAT-T6 and DTAT-T7 A356.0-Type Al-Si-Mg Alloy at 105^0C from the weight loss plot Data in Simulated Seawater Environment

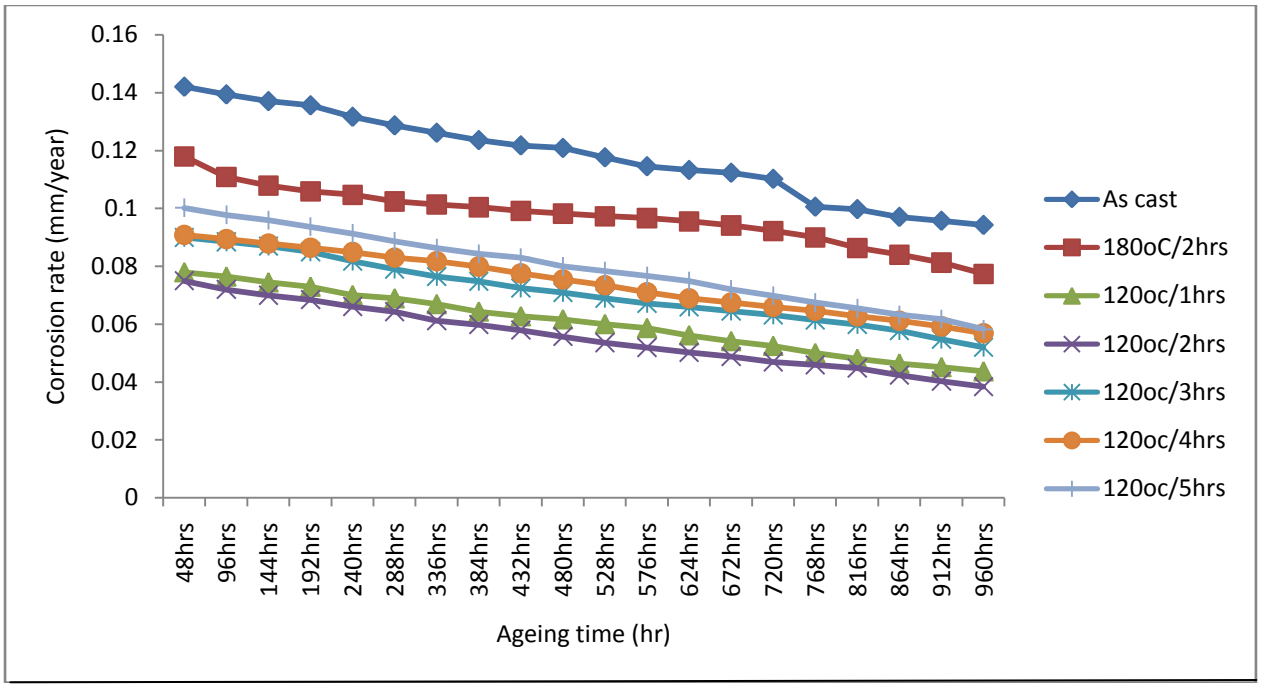


Figure 4.4: Variation of Corrosion rate with ageing time for As-cast, STAT-T6 and DTAT-T7 A356.0-Type Al-Si-Mg Alloy at 120^0C from the weight loss plot Data in Simulated Seawater Environment

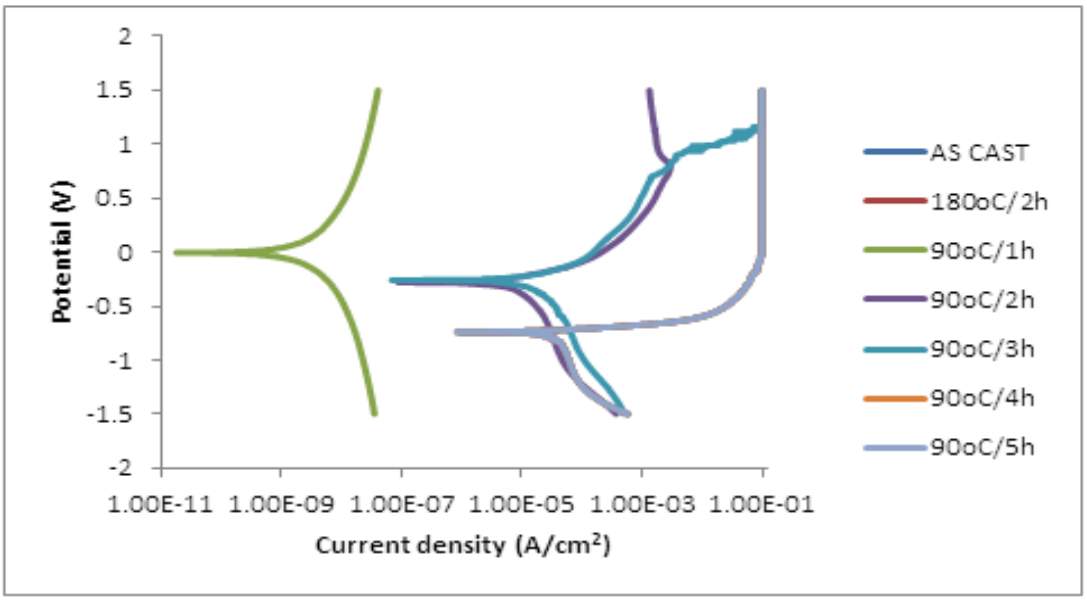


Figure 4.5: Potentiodynamic polarization curves of thermally pre-aged Al-Si-Mg alloy at 90^0C in 3.5% NaCl solution at 25^0C

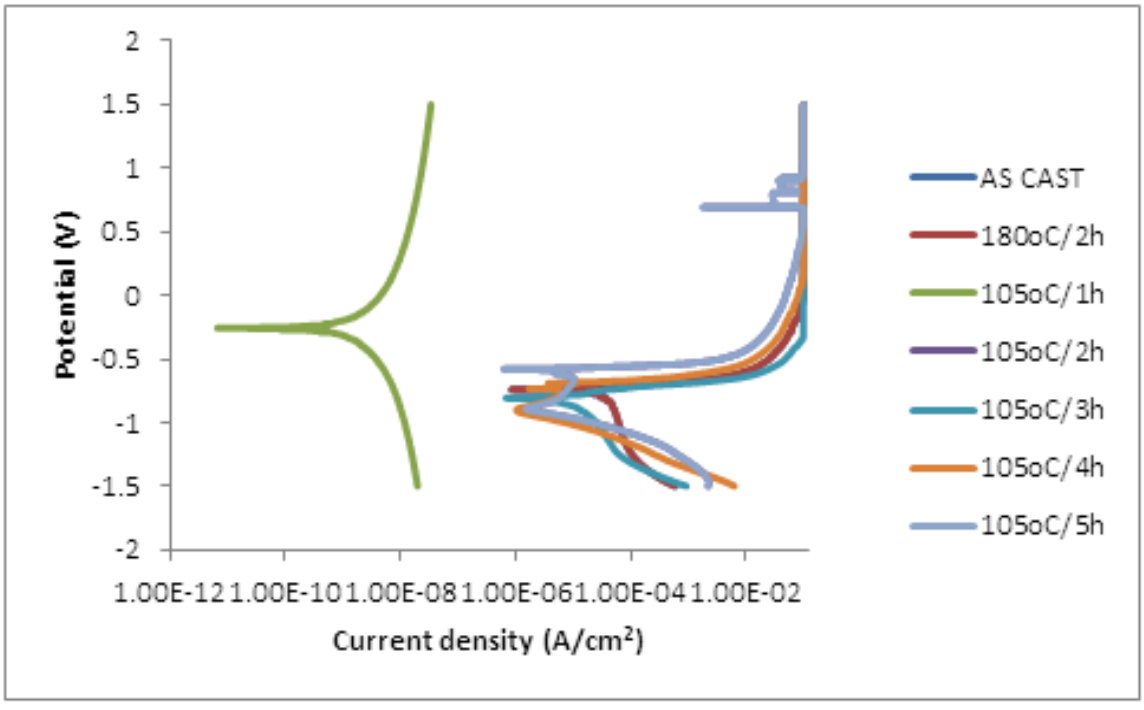


Figure 4.6: Potentiodynamic polarization curves of thermally pre-aged Al-Si-Mg alloy at 105^0C in 3.5% NaCl solution at 25^0C

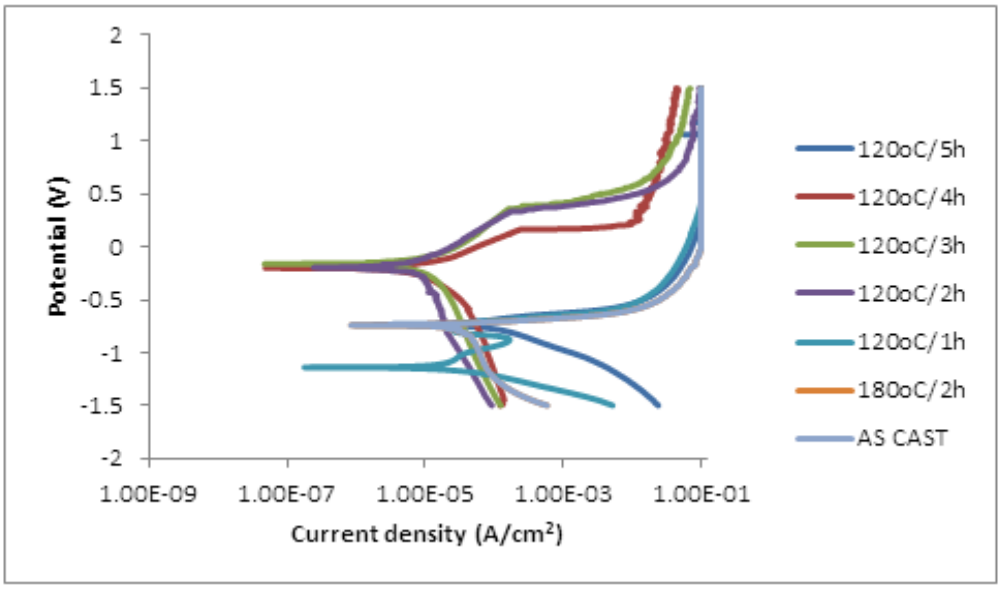


Figure 4.7: Potentiodynamic polarization curves of thermally pre-aged Al-Si-Mg alloy at 120^{0}C in 3.5% NaCl solution at 25^{0}C

Fig.8-9 show X-ray Diffractometry pattern A356.0-Al-Si-Mg Alloy for the As-cast and double thermally aged at 90^{0}C/2hrs

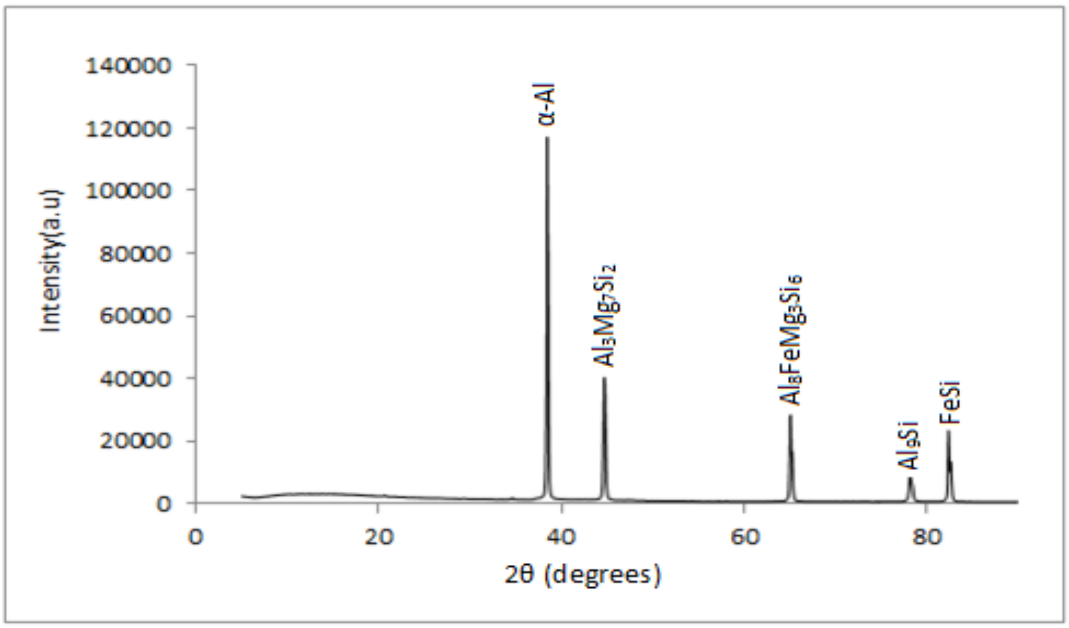


Figure 4.8: XRD Pattern A356.0-type Al-Si-Mg Alloy for As Cast

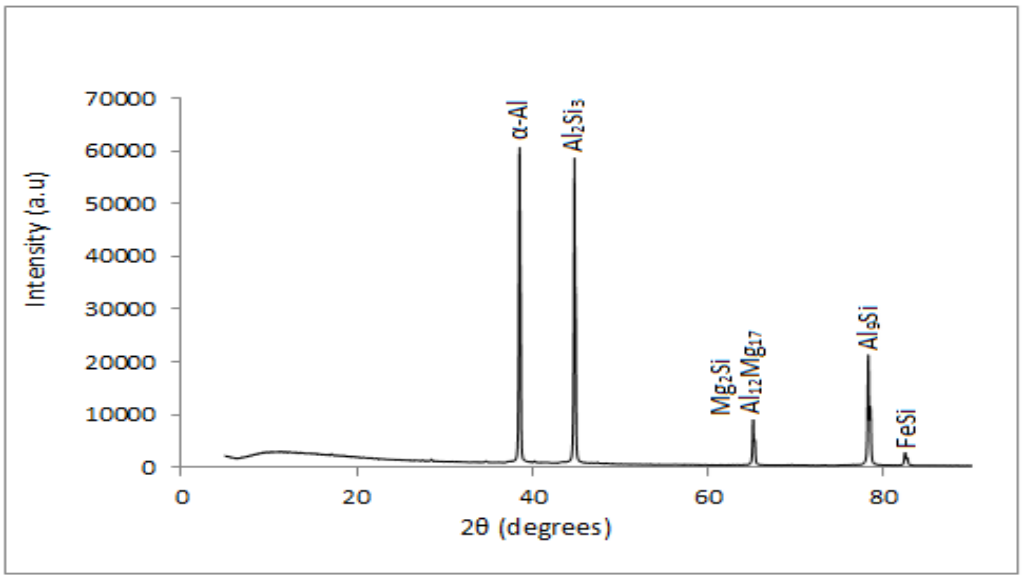


Figure 4.9: XRD Pattern of Thermally Treated A356.0-type Al-Si-Mg Alloy after DTAT (90^0C/1hr) showing phases present.

Plates I-VII show the SEM/EDS for the as-cast and DTAT 90^0C/2hrs, OPM of the as-cast and antimony modified Al-Si-Mg alloy and OPM of as-corroded at selected days

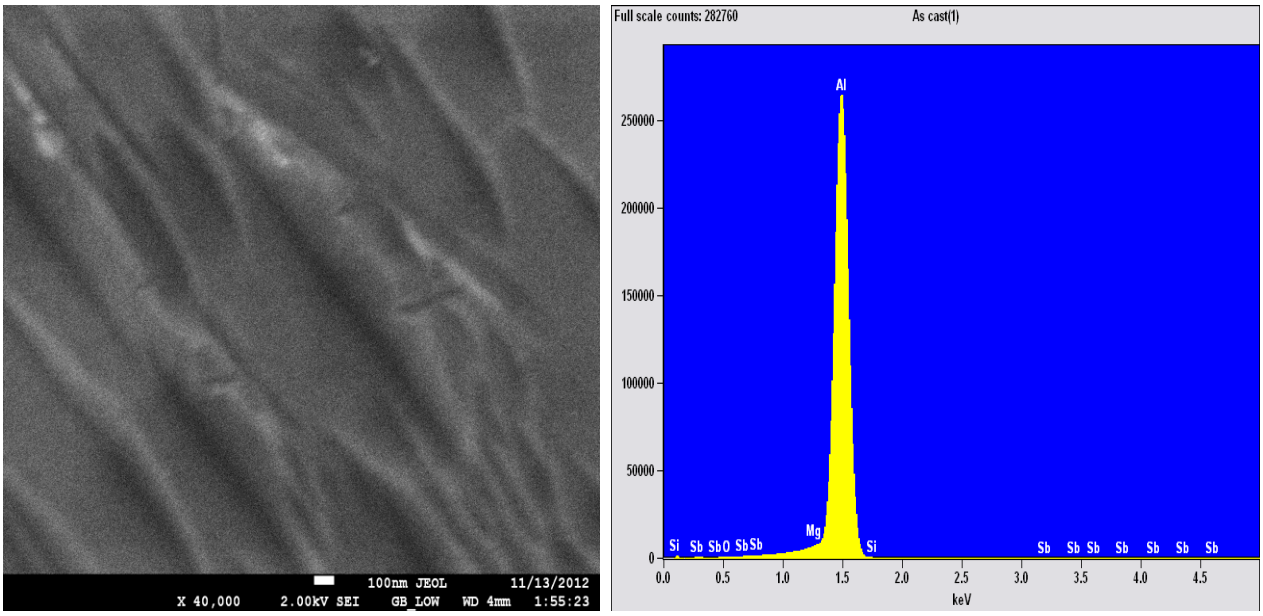


Plate I: SEM micrograph with the EDS spectrum of the As-cast sample

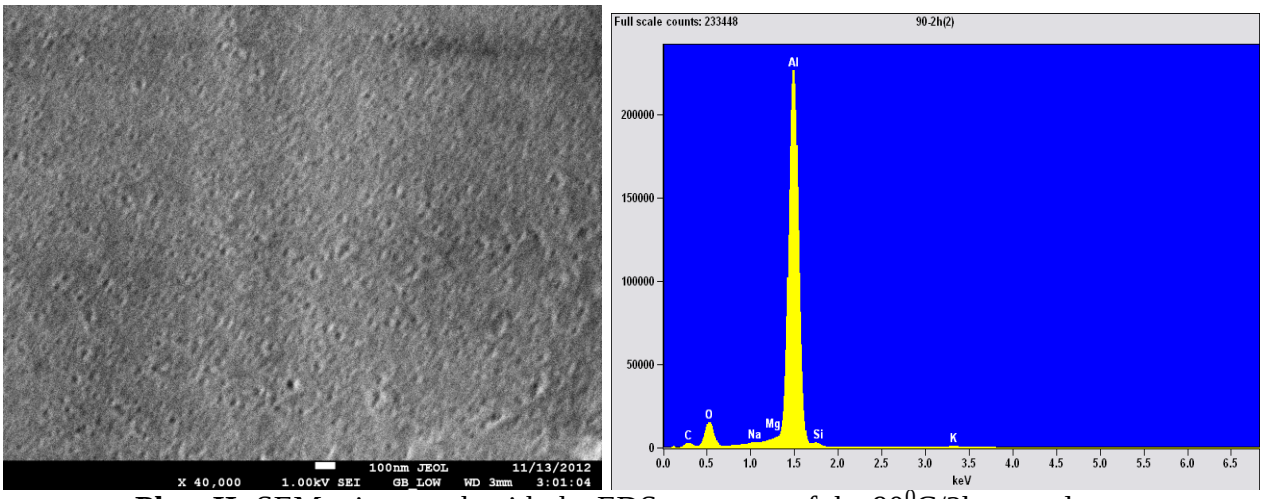


Plate II: SEM micrograph with the EDS spectrum of the 90^0C/2hr sample

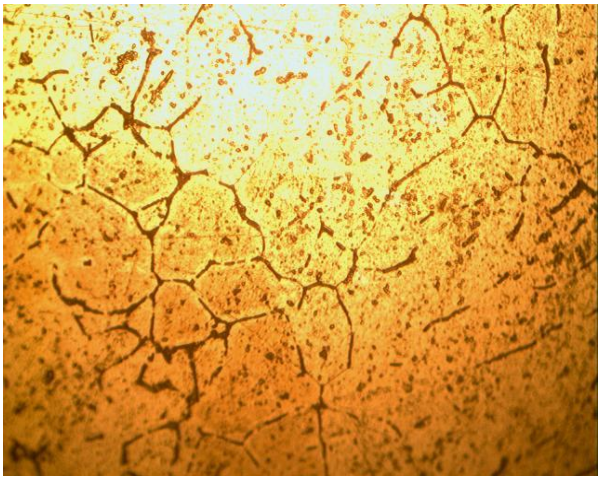


Plate III: OPM As cast Structure Al-Si-Mg alloy × **100**

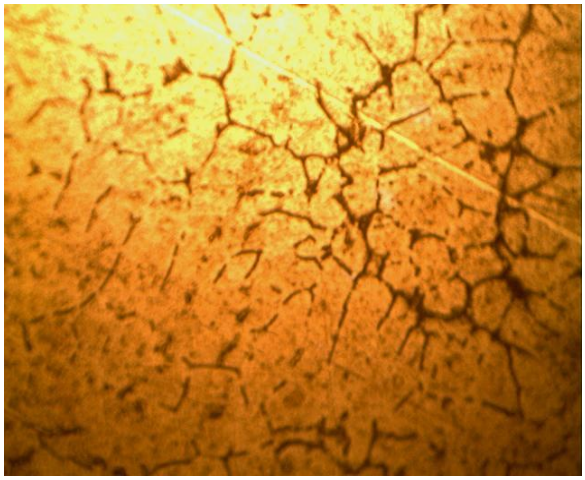


Plate IV: O PM of Antimony Modified Al-Si-Mg alloy × **100**

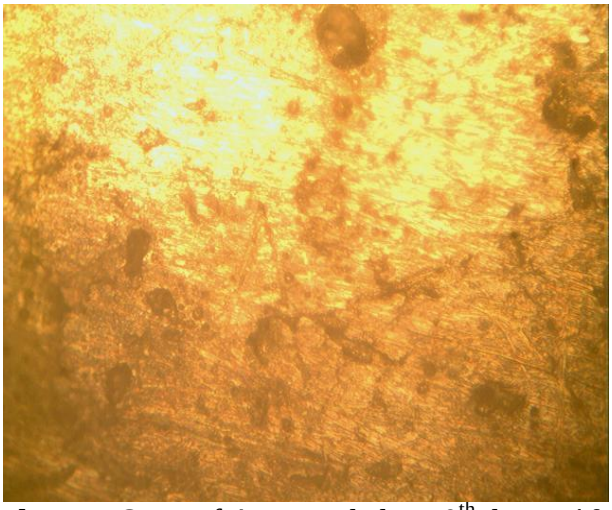


Plate V: OPM of As corroded at 20th day × **100**

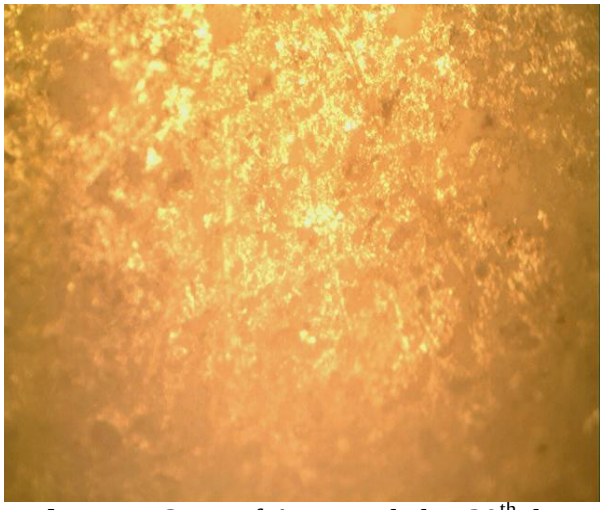


Plate VI: OPM of As corroded at 30th day × **100**

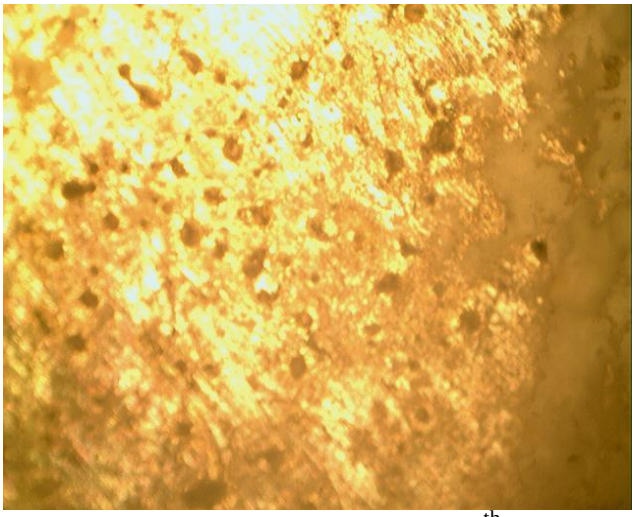


Plate VII: OPM of As corroded at 40th day showing susceptibility to pitting corrosion × **100.**

CHAPTER FIVE

5.0 DISCUSSIONS

5.1 Hardness Measurement and Thermal Ageing Treatments

5.1.1 *Single Thermal Ageing (STAT) and Double Thermal Ageing (DTAT) Treatments*

Hardness tests have been performed to evaluate the hardness of As-cast, STAT and DTAT. Three measurements were performed on each As-Cast, STAT and DTAT comprising 90^0C/1-5hr, 105^0C/1-5hr and 120^0C/1-5hr, so as to obtain average hardness value that could be more accurate to represent the hardness property of specimen.

Table 4.1 presents the average hardness value for the alloy, the result of STAT shows an increase in hardness (6.13HRF), while the DTAT increases the hardness up to 8.40HRF at 90^0C/2hr (Figure 4.1) as the peak ageing temperature and time for the alloy studied. Beyond the peak hardness, the hardness value decreased. The reason could be as a result of the fact that any decrease in hardness associated with an increase in the inter-particle spacing between precipitates, which makes dislocation bowing much easier (Abdulwahab *et al.,* 2011).At peak hardness temperature, the microstructure have been refined by the heat treatment into a fine dispersion of $Al_{12}Mg_{17}$, $Al_8FeMg_3Si_6$, $Al_3Mg_7Si_2$ strengthening phases (Abdulwabab *et al.,* 2011) which is coherent along with the semi-coherent clusters. The alloy at this peak ageing temperature and time (Figure 4.1) produces hardness value that is attributed to formation of Mg_2Si and other strengthening phases as observed by (Pio, 2011; Hurtalova' *et al.,* 2012 ;Abdulwahab *et al.,* 2011).The precipitation constituent as stated by Pio (2011) accounted for an increased in hardness, been that the eutectic Si transformed into spheroidized eutectic Si embedded among the homogeneous α-Al matrix. Figure 4.2 shows samples pre-aged at temperature 105°C, an increased in hardness to the aging peak after 3hours, followed by a decrease in hardness which increases again and reaches the potential second peak after 5 hours. The early stage of aging for temperature 120°C at 1hour was measured (Figure 4.3). The second aging peak for temperature 120°C at 3hours was observed. The age-hardening peaks are correlated to their precipitation

sequence. The first hardness peak of age hardening curve is attained depending on the high density GP zones (especially GP II zones), while the second one is acquired in terms of metastable particles. The aging at 90^0C corresponds to the continuous transition from GP zones to metastable phases as observed in the work of Hurtalova' *et al.*, (2012).

5.2.1 Relationship between Microstructure and Hardness Characteristics of the studied Al-Si-Mg alloy

The unmodified alloy contains silicon in the form of brittle flakes which leads to poor ductility, but the antimony addition change the second phase of the elements by enhancing its growth and hardness (Sarada *et al.,* 2013). The as-cast microstructure consists of α-aluminium solid solution with the antimony modified eutectics (plate III and IV).Within the α-aluminium solid solution, the intermetallic phases consisting of several precipitates. These intermetallic phases are shown by the SEM and the XRD study. However, the strengthening phases such as Al_2Si_3, Mg_2Si, $Al_3Mg_7Si_6$, $Al_{12}Mg_{17}$, Al_9Si, and FeSi were reported by the XRD spectrum for the as-cast and the DTAT (90^0C/2hr) (Plate I and II).The as- cast revealed the presence of silicon flakes while the DTAT structure consist of spherodized silicon particles and refined grains. The Mg_2Si dispersiod phase is more refined, highly populated and distributed within the matrix of aluminium solid solution. These have been shown in the SEM secondary back scattering electron images (Plate II).In the microstructure, it is clear that more fine precipitate of β" dispersion occurred from the pre-ageing stage of the alloy, similar to those observed in (Lizi *et al.,* 2010;Abdulwahab *et al.,* 2011).This may be responsible for the improved hardness.

5.2.2 Corrosion Characteristics

5.2.2.1 Potentiodynamics Linear Polarization, STAT and DTAT treatment

Figures 4.4-4.6 show the potentiodynamics scanning curves and the corresponding corrosion parameters of As-cast, STAT and DTAT for A356.0-type Al-Si-Mg alloy in a 3.5wt% NaCl. The corrosion rate of all the samples studied showed a smaller passive region (cathodic) and prolong active region (anodic).Observations from the results indicated that the corrosion rates are very

similar in trend for all the examined samples irrespective of the treatment. This is because the samples were from the same alloy which was cast and solidified in similar conditions of cooling rate. However, the corrosion rate increases with increasing ageing time (Figures 4.7-4.9) for all the DTAT samples. This is in agreement with those reported (Osorio *et al.*, 2007; Andreatta *et al.*, 2004; Abdulwahab *et al.*, 2011; Abdulraham and Aigbodion, 2006). It can be clearly seen that the corrosion potential at 90^0C/5hr is the most positive and same with those of as-cast and STAT samples, while at 90^0C/1hr is the most negative, Tables 4.5-4.7 and Figures 4.7-4.9.The polarization Resistance (Rp) at 105^0C/1hr is highest. These results indicated that the particles of aluminum alloy A356 at STAT condition are more susceptible to corrosion than DTAT at all ageing temperatures and time; because of it low polarisation potential and current density when compared to that of DTAT. The reason for the high corrosion resistance of the DTAT samples is due to the fact that, DTAT promotes coarse precipitates of the equilibrium phase of β-Mg_2Si in the grains and sub-grains boundaries, while maintaining a fine distribution of β' in the grain interiors. These coarse intermetallic particles then act as hydrogen trapping sites, locally reducing the hydrogen concentration in the matrix around the grain boundary (Hughes *et al.*,2011; Reda *et al.*, 2008). Figures 4.5-4.7 show the current densities (corrosion rate) and their corresponding corrosion potential. From the hardness measurement, it is expected that samples with higher HRF value should have greater corrosion rate. Since at higher HRF value, grain size of the sample is finer and such structures are more susceptible to corrosion than the coarse ones; especially when the precipitate on the grain boundaries of the alloys becomes coarser (Abdulwahab *et al.*, 2011).But this did not hold for the studied samples in this work. The phases formed Figure 4.10 which enhanced hardness may probably have some deleterious effect on the physiochemical properties of the alloy in the electrochemical polarization condition. The ageing temperatures and the degree of supersaturation played a major role in the final properties of the alloy. However, as the ageing progresses, the inter-atomic spacing and the bond between the molecules changed which account for the electrochemical behavior of these samples. Such tendency agreed with the

results obtained (Abdulwahab *et al.*, 2011,Osorio *et al.*, 2007).The corrosion resistance of A356.0-type Al-Si-Mg alloy studied seems to be strongly associated not only with the distribution of eutectics which is dependent on the interdendritic spacing, but also with the fineness of the eutectic inter-phase spacing. Comparatively, samples aged at 105^0C for 1hr at DTAT exhibit the highest corrosion resistance in 3.5wt% NaCl solution considered in this work.

5.2.3 Microstructure and Degradation of Al-Si-Mg alloy after Electrochemical Corrosion Attack

Plate III is the as-cast microstructures of Al-Si-Mg alloy. These images show four types of intermetallic compounds $Al_3Mg_7Si_6$ (Hexagonal), $Al_{12}Mg_{17}$ (Cubic), Al_9Si, FeSi (Cubic) located at the grain boundaries. Since it is difficult to produce detailed identification of intermetallic using only microscopic examination, XRD technique was utilized to provide confidence in the results of phase classification based on metallographic study (Figure 4.8-4.9).

As-cast SEM image shows a uniform fringe contrast indicating presence of silicon flakes (Plate I). No contrast which can be attributed to the precipitates is observed as described in similar SEM of (Murayama and Hono, 2007). Plate II illustrate the SEM for the 90^0C/2hr.White contrasts arise from extremely fine particles precipitated homogeneously in Al matrix. The shape of these fine precipitates is not well-defined since they are very fine and the selected area diffraction pattern shows neither extra reflection nor diffuse scattering, which suggested that these precipitates are fully coherent with matrix and have not any distinct structure. Lizi *et al.*, (2010) attributed the precipitates as spherical Guinier Preston (GP) zones.

The high corrosion resistance of the alloy at DTAT may not be unconnected with the presence of many aluminum containing intermetallics and only one iron containing intermetallic (FeSi). Hughe *et al.*, (2011) stated that the surface of Al-Si-Mg alloy may contain either mixed Al-Mg oxide regardless of the alloy type. This is primarily because of the heat of segregation of Mg is high and it has a favourable free energy for the formation of the oxides. Since Aluminium readily

oxidizes both in intermetallic particles as well as from the matrix, oxides formed would be relatively protective.

CHAPTER SIX

6.0 SUMMARY, CONCLUSION AND RECOMMENDATIONS

6.1 Summary

The effect of pre-aging thermal conditions on the hardness, corrosion resistance and microstructural morphology of antimony modified Al-Si-Mg alloy has been studied. The temper conditions are T6 and T7, while the thermal treatments are STAT and DTAT. The possible strengthening phases of the treated samples were identified by XRD spectrum as Al_9Si, Al_3Si_3, Mg_2Si, $Al_{12}Mg_{17}$ and FeSi. The corrosion characteristics of the treated alloy were evaluated using weight loss and linear polarization methods. From the results (Figures 4.2- 4.7), the treated samples in the STAT and DTAT showed an improvement in the hardness of the alloy. But the DTAT showed better hardness than the convectional STAT condition, except at 120^0C/4hr and 120^0C/5hr. The DTAT treatment increased the alloy hardness by 67.0% as compared with 21.9% increase in alloy hardness by the STAT treatment. Considering thermal treatments, sample aged at 90^0C in the DTAT condition as been observed to be the peak aged alloy at 2hr (8.40HVN) of ageing time. The corrosion of the DTAT treated alloy in the simulated sea water showed higher improvement in the corrosion resistance than the STAT treated alloy. The corrosion damaged can be attributed to pitting corrosion. In summary, the modifier (antimony) and DTAT treatment have positive improvements on the hardness value (67.0%) and corrosion resistance of samples considerably.

6.2 Conclusion

In this research, variation in pre-ageing conditions of the DTAT samples has greatly improved the hardness value to 67% as a result of a low temperature ageing at 90^0C for 2 h. However, significant results have been obtained with higher corrosion resistance in the DTAT-temper condition than the STAT temper. In line with the above, the following conclusions are made;

- ✓ The results show that using antimony as modifier and DTAT treatments with varying pre-ageing thermal treatment improved the hardness value of Al-Si-Mg alloy within the studied pre-ageing temperatures and times.
- ✓ The peak hardness value of 8.40HRF was achieved from DTAT treatment which comprised a low temperature ageing at 90^0C for 2hrs, followed by ageing at 180^0C for 2hrs. The hardness of 6.13HRF was obtained at 180^0C after 2hrs of ageing is lower than those obtained by other DTAT treatments.
- ✓ The DTAT treatment improvement on the alloy hardness can be attributed to the fine dispersion of precipitates obtained as a result of the pre-ageing treatment, which was retained and fully transformed to finer particles at 180^0C for 2hrs.
- ✓ The results of weight loss of Al-Si-Mg alloy in simulated sea water environment has shown that the corrosion resistance of DTAT Al-Si-Mg alloy has been enhanced significantly as compared to those observed in the STAT condition.
- ✓ The results of the linear polarization indicated that DTAT treatment has greatly improved the corrosion resistance of samples at all the pre-ageing temperatures and time as compared with the STAT.

6.3 Recommendation

1. Study should be made on the phase and crystal orientation of the alloy during ageing.
2. The use of Transmission electron microscope (TEM) is recommended for the study of GP-Zones in antimony modified Al-Si-Mg alloy.
3. The effect of DTAT on the studied antimony modified Al-Si-Mg alloy using thixocasting or other production route is recommended

REFERENCE

Abdulwahab, M., Madugu, I.A, Yaro, S.A, & Popoola, A.P.I (2012). Effects of Temper Conditions and Step-Quenching-Ageing on the Hardness Characteristics and Yield Strength of A356.0-type Al-Si-Mg Alloy. *Silicon , 4* (2), 137-142.

Abdulwahab, M., Madugu, I.A, Yaro, S.A, & Popoola, A.P.I (2011). Degredation Behavior of High Chromium Sodium-Modified A356.0-Type Al-Si-Mg Alloy in Simulated Seawater Environment. *Journal of Materials and Materials Characterization and Engineering , 10* (6), 535-551.

Abdulwahab, M., Madugu, I.A, Yaro, S.A, Hassan, S.B, & Popoola, A.P.I (2011). Effects of multiple-step thermal ageing treatment on the hardness characteristics of A356.0-type Al–Si–Mg alloy. *Materials and Design , 32*, 1159-1165.

Alcan. (2007, April). *www.kandhprecision.com/media/Alcan prime alloys*. Retrieved from www.kandhprecision.com.

Al-Helal, K.W.A. (2013). New Approaches to Casting Hypereutectic Al-Si Alloys to Achieve Simultaneous Refinement of Primary Silicon and Modification of Eutectic Silicon. *Ph.D Thesis* , Brunel Centre for Advanced Solidification Technology (BCAST), Brunel University.

Andreatta, F., Terryn, H., & de Wit, J. (2004). Corrosion Behaviour of Different Tempers of AA7075 Aluminum Alloy. *Electrochimica Acta , 49*, 2851,2862.

Selvaduray, G. (2004). *Ternary Phase Diagrams: Introduction.*San Jose State University.

Apelian, D. (2009). *Aluminum Cast Alloys:Enabling Tools for Improved Performance.* Illinois: NADCA.

ASM. (1984). *Heat Treating* (9 ed., Vol. 4). OH: Metal Park.

Avcorp. (2012). *Avcorp's Heat Treatment of Aluminum*. (Avcorp Industries Inc.) Retrieved from www.avcorp.com.

Blankenship, C., StarkeE.A., & Hornbogen, E. (1992). *Aluminum Alloys - Their Physical and Mechanical Properties* (Vol. 3). Norway: Trondheim.

Boontein, S., Kajornchaiyakul, J., & Limmaneevichitr, C. (2008). Effect of Alloying Element Antimony on Macrostructural and Microstructural Development in A356 Alloy Directionally Solidified under Unsteady-state Conditions. *Journal of Materials Science and Technology , 24* (1), 25.

Caia, Y., Liangb, R., Houa, L., & Zhanga, J. (2011). Effect of Cr and Mn on the Microstructure of Spray-Formed Al–25Si–5Fe–3Cu Alloy. *Materials Science and Engineering A , 528*, 4248.

Callister W.D, J. (2001). *Fundamentals of Materials Science and Engineering.* New York: John Wiley & Sons, Inc.

Chen, Z., Ma, C., & Chen, P. (2012). Eutectic Modification of A356 Alloy with Li Addition Through DSC and Miedema Model. *Transactions of Nonferrous Metals Society of China* , 42.

Comalco. (1997). *Modification of FoundryAl-Si Alloys.* Australia: Comalco Aluminium Limited.

Davis, J. (2000). *Corrosion:Understanding the Basics.* Ohio: ASM International.

Di Sabatino, M. (2005). Fluidity of Aluminum Foundry Alloys. *Ph.D Thesis* , 25. Norway: Norwegian University of Science and Technology.

Di Sabatino, M., Syverstsen, F., Arnberg, L., & Nordmark, A. (2005). An Improved Method for Fluidity Measurement by Gravity Casting of Spirals in Sand Moulds. *International Journal of Casting Metals Research , 18*, 59-62.

Durmus, H., & Meric, C. (2007). Age-hardening Behavior of Powder Metallurgy AA2014 Alloy. *Materials and Design , 28*, 982.

Erhard, O. (2002). Development of Al-Si-Mg Alloys for Semi-Solid Processing and Silicon Sphroidization Treatment of Al-Si Cast Alloy. *Ph.D Thesis* , 13-16. Zurich: Federal Instituteof Technology.

Ernst, F. (2004). *Precipitation Hardening of Al–Si–Mg Alloys.* Spring Semester.

Escalera-Lozano, R., Pech-Canul, M., Pech-Canul, M., Montoya-Dávila, M., & Uribe-Salas, A. (2010). The Role of Mg2Si in the Corrosion Behavior of Al-Si-Mg Alloys for Pressureless Infiltration. *The Open Corrosion Journal , 3*, 73-79.

Fontana, M., & Greene. (1987). *Corrosion Engineering* (3 ed.). New York: McGraw-Hill Book Company.

Gbenebor, O., Abdulwahab, M., Fayomi, O., & Popoola, A.P.I (2012). Influence of Inoculant Addition and Cooling Medium on the Mechanical Properties of AA6063-Type Al-Mg-Si Alloy. *Chalcogenide Letter , 9* (5), 201.

Gitter. (2008). Design of Aluminium Structure:Selection of Structural Alloys. *structural Design According to Eurocode9:Essential of Properties of Materials and Background Information* (pp. 2-12). Brussel: EUROCODES.

MHB. (1990). *Properties and Selection:Nonferrous Alloy and Specia- Purpose Materials* (Vol. 2). ASM International Handbook Company.

Hassan, S.B, & Aigbodion, V.S (2009). The effect of Thermal Ageing on Microstructure and Mechanical Properties of Al-Si-Fe/Mg Alloys. *Journal of Alloys and Compounds , 486*, 309-314.

Hirth, S., Marshal, G., & Lloyd, D. (2001). Effect of Si on the Behaviour and Formality of Aluminum Alloys based on AA6016. *Materials Science and Engineering A , 319* (321), 452.

Hitchcock, M., Wang, Y., & Fan, Z. (2007). Secondary Solidification Behavior of the Al-Si-Mg Alloy prepared by the Rheo-Die Casting Process. *Acta Materialia , 55*, 1589-1591.

Hong, Y., Yong, H., & Xiao-qian, W. (2010). Influence of Sb Modification on Microstructures and Mechanical Properties of Mg2Si/AM60 Composite. *Transactions of Nonferrous Metals Society of China , 20*, 411-415.

Hughes, A. E., Birbilis, N., Mol, J., Garcia, S., Zhou, X., & Thompson, G. E. (2011). High Strength Al-Alloys: Microstructure, Corrosion and Principles of Protection. In Zaki, A, *Recent Trends in Processing and Degradation of Aluminium Alloys* (pp. 223-254). Slavka Krautzeka , Rijeka, Croatia: InTech.

Hurtalova', L., Belan, J., Tillova', E., & Chalupova', M. (2012). Changes in Structural Characteristics of Hypoeutectic Al-Si Cast Alloy. *MATERIALS SCIENCE (MEDŽIAGOTYRA) , 18* (3), 228-232.

Imurai, S., Chaiyaku, K., Pearce, J., & Chairuangsri, T. (2010). Age Hardening and Precipitation Behaviour of an Experimental Cast Al-Mg-Si Alloy Treated by T6 and T616 Heat Treatment. *Chiang Mai Journal of Science , 37* (2), 269.

Jacobs, M. (1999). Precipitation Hardening. *TALAT Lecture:Interdisciplinary Research Centre in Materials The University of Birmingham,UK,1204*, 2-10.European Aluminium Association.

Jaukovic, N., & Asanovic, V. (2006). Effect of Temper and Chemical Composition on Polarization Resistance of Aluminum RR58 alloy. *Journal of materials and Processing Technology , 174*, 293-295.

Jenabali, S., Dehghan, A., & Malekjani, S. (2004). Effects of Optimum Amount of Sr and Sb Modifiers on Tensile,Impact and Fatigue Properties of A356 Aluminum Alloy. *Iran Journal of Science and Technology,TransactionB , 28* (B2), 225.

Jiang, X., He, G., Liu, B., Fan, S., & Zhu, M. (2011). icrostructure-Based Analysis of Fatigue Behavior of Al-Si-Mg Alloy. *transactions of Nonferrous Metals Society of China , 21*, 443.

Key to Metals. (2010). Retrieved June 15, 2012, from www.keytometals.com.

Kezhun, H., Fuxiao, Y., Dazhi, Z., & Liang, Z. (2011). Microstructural Evolution of Direct Chill Cast Al-15.5Si-4Cu-1Mg-1Ni-0.5Cr Alloy During Solution Treatment. *Research and Development .China Foundry , 8* (3), 264.

Kosgey, B., Maube, S., Wangombe, D., Maranga, S., & Kihiu, J. (2011). Effects of addictives on the Fatigue and Impact Properties of Recycled Al-Si Alloy Wheels. 1-4. Nairobi, Kenya: Jomo Kenyatta University of Agriculture and Technology.

Kumar, G., Hegde, S., & Prabhu, N. (2007). Heat Transfer and Solidification Behavior of Modified A356 alloy. *Journal of Materials Processing Technology , 182*, 152.

Kuntongkun, S., Plookphol, T., & wannasin, J. (2008). Influence of Heat treatment Processing parameters on the Hardness and the Microstructure of Semi-Solid Aluminum Alloy A356. *Journal of Metals,Materials and Minerals , 18* (2), 93.

Leo, P., & Cerri, E. (2003). Silicon Particle Damage in a Thixocast A356 Aluminum Alloy. *Metallurgical Science and Technology , 21* (1), 27.

Li, J., Peng, Z., Li, C., Jia, Z., Chen, W., & Zheng, Z. (2008). Mechanical Properties,Corrosion Behaviours and Microstructures of 7075 Aluminum Alloy with various Aging Treatments. *Transactions of Nonferrous Metals Society of China , 18*, 756-762.

Li, Y., Brusethaug, S., & Olsen, A. (2006). Influence of Cu on the Mechanical properties and Precipitate Behavior of AlSi7Mg0.5 Alloy During Ageing Treatment. *Scripta Materialia , 54*, 99.

Liu, G. (2009). Effect of Ageing Heat Treatment on Hardness and Tensile Properties of Aluminum A365.2 Casting Alloy. *Thesis* , 26. Ontario: Mc Master University Hamilton.

Lizi, H.,Haitao, Z., & Jianzhong, C. (2010). Effects of Pre-Ageing Treatment on Subsequent Artificial Ageing and Characteristics of an Al-1.01Mg-0.68Si-1.78Cu Alloy. *Journal of Material Science and Technology , 2*, 141-144.

Masuda, T., Takaki, Y., Sakurai, T., & Hirosawa, S. (2010). Combined Effect of Pre-Straining and Pre-Aging on Bake-Hardening Behaviorof an Al-0.6 mass%Mg-1.0 mass%Si Alloy. *Materials Transactions, , 51* (2), 325-331.

Moldovan, p., Popescu, G., & Butu, M. (2007). Heat Treatment of Al-7Si--0.3Mg Alloy Previously Inoculated with a New Type of Quarternary Master Alloy. *U.P.B Sciences Bulletin,Series B , 69* (2), 91.

Moller, H., Govender, G., & Stumpf, W. (2008). The T6 Heat Treatment of Semi-Solid Metal Processed Alloy A356. *The Open Materials Science Journal , 2*, 6.

Morri, A. (2010). Emperical Models of Mechanical Behavior of Al-Si-Mg Cast Alloys for High Performance Engine application. *Metallurgical Science and Technology , 28* (2), 3.

Nestor, P. (2004). *Electrochemistry and Corrosion Science.* New York: Kluwer Academic Publishers.

Omotoyinbo, J., & Oladele, I. (2010). The Effect of Deformation and Magnesium Content on the Mechanical properties of 6063 aluminum Alloys. *Journal of Materials and Materials Characterization and Engineering , 9* (6), 540.

Osorio, W., Spinelli, J., Freire, C., Cardona, M., & Garcia, A. (2007). The Role of Al2Cu and of Dendritic Refinement on surface Corrosion Resistance of Hypoeutectic Al-Cu Alloys Immersed in H2SO4. *Journal of Alloys and compounds , 443*, 87-93.

Peng, J., Tang, X., He, J., & Xu, D. (2011). Effect of heat treatment on microstructure and tensile properties of A356 alloys. *Transactions of Nonferrous metals Society of China , 21*, 1950.

Perez, G. (2011). *alerter@rdpartners.net*. (European R&D Partner Search) Retrieved from www.aimen.es.

Pio, L. (2011). Effect of T6 Heat Treatment on the Mechanical Properties of Gravity Die Cast A356 Aluminum Alloy. *Journal of Applied Sciences* , 1-2.

Rana, R.S., Purohit, R., & Das, S. (2012). Reviews on the Influences of Alloying elements on the Microstructure and Mechanical Properties of Aluminum Alloys and Aluminum Alloy Composites. *International Journal of Scientific and Research Publications ,2(6),*1-6

Reda, Y., Abdel-Karim, R., & Elmahallawi, I. (2008). Improvement in Mechanical and Stress Corrosion Cracking properties in Al-alloy 7075 via Retrogression and reaging. *Materials Science and Engineering A , 485*, 468-472.

Reddy, G., & Rao, K. (2010). Enhancement of Wear and Corrosion Resistance of Cast A356 Aluminum Alloy using Friction stir Processing. *Transactions of the India Institute of Metals , 63*, 793.

Roberge, P. (1999). *Handbook of Corrosion Engineering.* New York: McGraw-Hill Companies.

Sarada, B, N., Srinivasamurthy, P.L., & Swetha (2013).Microstructural Characteristics of Sr and Sodium Modified Al-Mg-Si alloy. *International Journal of Innovative Research in Science, Engineering and Technology*, 2(8), 3978-3983

Schweitzer, P. (2007). *Corrosion Handbook:Fundamentals of Metallic Corrosion* (2 ed.). Boca Raton: CRC Press.

Shuhui, M. (2006). A Methodology to Predict the Effects of Quenching rates on Mechanical Properties of Cast AluminumAlloys. *PhD Degree Thesis* . Worcester Polytechnics Institute.

Siriporn, K., Sirikul, W., Thawatchai, P., & Jessada, W. (2008). Influence of Heat Treatment processing Parameters on the Microstructure of Semi-Solid Aluminum Alloy A356. *Journal of Metals,Materials and Minerals , 18* (2), 93.

Tahamtan, S., & Boostani, A. (2010). Microstructure Characteristics of Thixoforged A356 Alloy in Mushy State. *Transactions of Nonferrous and Materials Society of China , 20*, 781.

Tash, M., Kalifa, W., & El Hashash, A. (2008). Effect of Metallurgical Differences Between 356 and 384 Alloys on their Mechanical Properties. *Proceedings on the Ninth Cairo University International Conference on Mechanical Design and Production* (pp. 993-1003). Cairo: MDP-9.

Tash, M., Samuel, F., Mucciardi, F., & Doty, H. (2007). Effect of Metallurgical Parameters on the Hardness and Microstructural Characterization of As-Cast and Heat-Treated 356 and 319 Aluminum Alloys. *Materials Science and Engineering A , 443*, 186,188.

Tavitas-Medrano, F., Gruzleski, J., Samuel, F., Valtierra, S., & Doty, H. (2008). Effect of Mg and Sr-Modification on Mechanical Properties of 319-type Aluminum Cast Alloys Subjected to Artificial Aging. *Materials Science and Engineering A , 480*, 356-357.

www.aleris.com. Thursday,June 21,2012,3:05a.m

www.avcorp.com.Friday,May 25,2012,9:45pm

www.aluminum.org.Sunday,May 27,2012,1:55pm

www.about.com.metals.Saturday,June 30,2012,2:24pm

www.alcotec.com.Sunday,June 24,2012,3:56pm

Xiao-Song, J., Guo-qiu, H., Bing, L., Song-Jie, F., & Min-hao, Z. (2011). Microstructure-Based Analysis of Fatigue Behavior of Al-Si-Mg Alloy. *Transactions of Nonferrous Metals Society of China , 21*, 443.

Zaki, A. (2006). *Principle of Corrosion Engineering and Corrosion Control.* Elsevier Science & Technology Books.

Zhang, Y., Ma, N., Le, Y., Li, S., & Wang, H. (2005). Mecchanical properties and Damping Capacity after Grain Refinement in A356 Alloy. *Materials Letters , 59*, 2174.

Zhen, L., & Kang, S. (1997). The Effect of Pre-aging on Microstructure and Tensile properties of Al-Mg-Si alloys. *Scripta Materialia , 36* (10), 1089-1093.

Zou, Y., Xu, Z., He, J., & Jianmi, Z. (2010). Crystallographic Characteristics of intermetallic Compound in Al-Si-Mg Casting Alloys by using Electron Backscatter Diffraction. *Chinese Journal of Mechanical , 23* (3), 1-2.

APPENDIX A

Table 4.5 Corrosion Rate of As-cast, STAT and DTAT (at 90^0C Preaging tempt.) in 3.5% NaCl Over exposure time (hours)

	Corrosion Rate in mm/yr																		
	48hrs	96hrs	144hrs	192hrs	240hrs	288hrs	336hrs	384hrs	432hrs	480hrs	528hrs	576hrs	624hrs	672hrs	720hrs	768hrs	816hrs	864hrs	912hrs	960hrs
As-cast	0.14204	0.13938	0.13705	0.13560	0.13164	0.12867	0.12612	0.12358	0.12174	0.12086	0.11763	0.11453	0.11324	0.11229	0.11019	0.10055	0.09972	0.09703	0.09569	0.09426
180^0C/2hr	0.11791	0.11086	0.10788	0.10590	0.10470	0.10241	0.10134	0.10041	0.09912	0.09822	0.09728	0.09667	0.09553	0.09412	0.09222	0.09001	0.08632	0.08404	0.08131	0.07741
90^0C/1hr	0.06703	0.06405	0.6242	0.06070	0.05887	0.05657	0.05389	0.05143	0.04927	0.04668	0.04553	0.04461	0.04317	0.04202	0.04127	0.04003	0.03953	0.03897	0.03670	0.03579
90^0C/2hr	0.07994	0.07745	0.07396	0.06820	0.06703	0.06546	0.06153	0.05821	0.05596	0.05396	0.05078	0.04821	0.04713	0.04553	0.04436	0.04346	0.04225	0.04046	0.04003	0.03890
90^0C/3hr	0.09298	0.09013	0.08904	0.08669	0.08434	0.08171	0.07890	0.07558	0.07305	0.06901	0.06703	0.06511	0.06349	0.06145	0.06013	0.05731	0.05588	0.05475	0.05337	0.05040
90^0C/4hr	0.09013	0.08845	0.08596	0.08171	0.07856	0.07446	0.07118	0.06876	0.06696	0.06436	0.06204	0.06005	0.05811	0.05645	0.05475	0.05201	0.05106	0.05005	0.04942	0.04553
90^0C/5hr	0.09388	0.09241	0.09192	0.08963	0.08594	0.08394	0.07809	0.07632	0.07494	0.07175	0.07001	0.06876	0.06686	0.06425	0.06207	0.06032	0.05895	0.05644	0.05347	0.05201

APPENDIX B

Table 4.6 Corrosion Rate of As-cast, STAT and DTAT (at 105^0C Preaging tempt.) in 3.5% NaCl Over exposure time (hours)

	Corrosion Rate in mm/yr																			
	48hrs	96hrs	144hrs	192hrs	240hrs	288hrs	336hrs	384hrs	432hrs	480hrs	528hrs	576hrs	624hrs	672hrs	720hrs	768hrs	816hrs	864hrs	912hrs	960hrs
As-cast	0.14204	0.13938	0.13705	0.13560	0.13164	0.12867	0.12612	0.12358	0.12174	0.12086	0.11763	0.11453	0.11324	0.11229	0.11019	0.10055	0.09972	0.09703	0.09569	0.09426
180^0C/2hr	0.11791	0.11086	0.10788	0.10590	0.10470	0.10241	0.10134	0.10041	0.09912	0.09822	0.09728	0.09667	0.09553	0.09412	0.09222	0.09001	0.08632	0.08404	0.08131	0.07741
105^0C/1hr	0.06016	0.05997	0.05797	0.05548	0.05278	0.05147	0.05009	0.04995	0.04798	0.04568	0.04261	0.04048	0.03896	0.03670	0.03511	0.03344	0.03174	0.03097	0.02844	0.02657
105^0C/2hr	0.06995	0.06797	0.06598	0.06323	0.06171	0.06007	0.05868	0.05647	0.05507	0.05371	0.05151	0.05022	0.04798	0.04568	0.04377	0.04188	0.04020	0.03846	0.03601	0.03344
105^0C/3hr	0.08493	0.08295	0.08171	0.07981	0.07706	0.07549	0.07403	0.07146	0.06896	0.06646	0.06523	0.06401	0.06142	0.05888	0.05857	0.05747	0.05419	0.05146	0.04896	0.04690
105^0C/4hr	0.08204	0.08044	0.07896	0.07546	0.07403	0.07246	0.07105	0.07003	0.06876	0.06706	0.06598	0.06421	0.06349	0.06204	0.05971	0.05825	0.05647	0.05475	0.05151	0.04821
105^0C/5hr	0.08918	0.08669	0.08434	0.08271	0.08044	0.07856	0.07632	0.07403	0.07175	0.06925	0.06703	0.06598	0.06449	0.06314	0.06204	0.06018	0.05811	0.05647	0.05371	0.05085

APPENDIX C

Table 4.7 Corrosion Rate of As-cast, STAT and DTAT (at 120^0C Preaging tempt.) in 3.5% NaCl Over exposure time (hours)

	Corrosion Rate in mm/yr																		
	48hrs	96hrs	144hrs	192hrs	240hrs	288hrs	336hrs	384hrs	432hrs	480hrs	528hrs	576hrs	624hrs	672hrs	720hrs	768hrs	816hrs	864hrs	912hrs	960hrs
As-cast	0.14204	0.13938	0.13705	0.13560	0.13164	0.12867	0.12612	0.12358	0.12174	0.12086	0.11763	0.11453	0.11324	0.11229	0.11019	0.10055	0.09972	0.09703	0.09569	0.09426
180^0C/2hr	0.11791	0.11086	0.10788	0.10590	0.10470	0.10241	0.10134	0.10041	0.09912	0.09822	0.09728	0.09667	0.09553	0.09412	0.09222	0.09001	0.08632	0.08404	0.08131	0.07741
120^0C/1hr	0.07794	0.07645	0.07446	0.07295	0.07006	0.06895	0.06696	0.06439	0.06276	0.06171	0.06007	0.05871	0.05621	0.05419	0.05254	0.05005	0.04808	0.04646	0.04522	0.04377
120^0C/2hr	0.07495	0.07201	0.06995	0.06845	0.06609	0.06431	0.06142	0.05983	0.05795	0.05575	0.05359	0.05195	0.05026	0.04881	0.04700	0.04596	0.04483	0.04240	0.04037	0.03846
120^0C/3hr	0.08991	0.08845	0.08695	0.08493	0.08171	0.07896	0.07644	0.07478	0.07246	0.07088	0.06894	0.06715	0.06595	0.06450	0.06314	0.06142	0.05988	0.05774	0.05475	0.05201
120^0C/4hr	0.09085	0.08943	0.08784	0.08644	0.08493	0.08302	0.08181	0.07995	0.07757	0.07549	0.07346	0.07105	0.06894	0.06754	0.06595	0.06463	0.06277	0.06123	0.05925	0.05689
120^0C/5hr	0.10017	0.09774	0.09591	0.09367	0.09130	0.08863	0.08631	0.08433	0.08297	0.07998	0.07830	0.07668	0.07495	0.07198	0.06983	0.06746	0.06550	0.06323	0.06167	0.05828